



**US Army Corps
of Engineers**
Waterways Experiment
Station

Technical Report CERC-93-10
June 1993

CERC LIBRARY

Dolos Design Procedure Based on Crescent City Prototype Data

by *Jeffrey A. Melby*
Coastal Engineering Research Center

WES

Approved For Public Release; Distribution Is Unlimited

The contents of this report are not to be used for advertising, publication, or promotional purposes. Citation of trade names does not constitute an official endorsement or approval of the use of such commercial products.



PRINTED ON RECYCLED PAPER

Dolos Design Procedure Based on Crescent City Prototype Data

by Jeffrey A. Melby
Coastal Engineering Research Center

U.S. Army Corps of Engineers
Waterways Experiment Station
3909 Halls Ferry Road
Vicksburg, MS 39180-6199

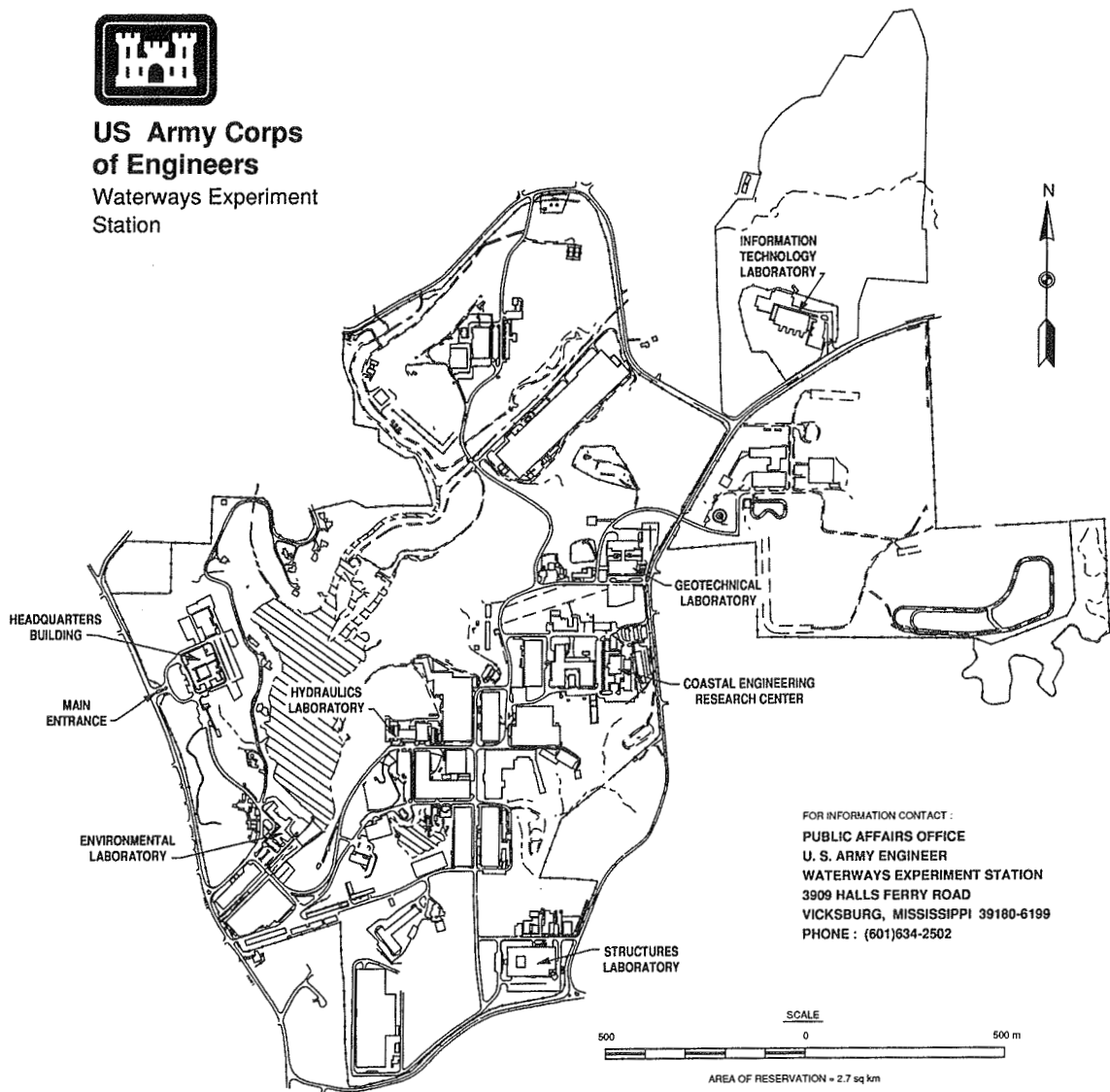
Final report

Approved for public release; distribution is unlimited

Prepared for U.S. Army Corps of Engineers
Washington, DC 20314-1000



**US Army Corps
of Engineers**
Waterways Experiment
Station



Waterways Experiment Station Cataloging-in-Publication Data

Melby, Jeffrey A.

Dolos design procedure based on Crescent City prototype data / by Jeffrey A. Melby, Coastal Engineering Research Center ; prepared for U.S. Army Corps of Engineers.

67 p. : ill. ; 28 cm. — (Technical report ; CERC-93-10)

Includes bibliographical references.

1. Breakwaters — Design and construction — Evaluation. 2. Structural analysis (Engineering) — Approximation methods. 3. Hydraulic models. 4. Hydraulic structures — Design and construction — Evaluation. I. United States. Army. Corps of Engineers. II. Coastal Engineering Research Center (U.S.) III. U.S. Army Engineer Waterways Experiment Station. IV. Title. V. Series: Technical report (U.S. Army Engineer Waterways Experiment Station) ; CERC-93-10.

TA7 W34 no.CERC-93-10

PREFACE

This study was conducted by the Coastal Engineering Research Center (CERC), US Army Engineer Waterways Experiment Station (WES). The work described herein was authorized as a part of the Crescent City Prototype Dolos Study, CERC. Messrs. John H. Lockhart, Jr. and Jesse Pfeiffer are Technical Monitors for Headquarters, US Army Corps of Engineers.

The Crescent City Dolos Structural Design Procedure Development was a task under the Crescent City Prototype Dolos Study, which was directly managed by Mr. Gary Howell, Prototype Measurement and Analysis Branch (PMAB), Engineering Development Division (EDD), CERC. The design development task study was performed and the report prepared over the period 1 October 1987 through 30 August 1990 by Jeffrey A. Melby, within the PMAB, from 1 October 1987 to 1 October 1989 and within the Wave Research Branch (WRB), Wave Dynamics Division (WDD), CERC from 1 October 1989 to 30 August 1990.

This report was reviewed, edited, and published under Civil Works Research Work Unit 32536, "Concrete Armor Unit Design," Coastal R&D Program, authorized by the USACE. The HQUSACE Technical Monitors were Messrs. John H. Lockhart, Jr.; John G. Housley; Barry W. Holliday; and David A. Roellig. Ms. Carolyn M. Holmes was the CERC Program Manager.

The research effort was conducted under the general administrative supervision of Dr. James R. Houston, Director, CERC, Mr. Charles C. Calhoun, Jr., Assistant Director, CERC, Mr. Gene Chatham, Chief, WDD, Mr. D.D. Davidson, Chief, WRB, Mr. Thomas Richardson, Chief, EDD, and Mr. William Preslan, Chief, PMAB.

The author gratefully acknowledges the dedicated efforts of the following people who helped during the study: Mr. Gary Howell, Dr. Steven Hughes, Mr. Thomas Kendall, Mr. Dennis Markle, Mr. D.D. Davidson, all with WES, Dr. Hans Burcharth, Prof. Leon Borgman, Prof. William McDougal, and Dr. Joseph Tedesco.

At the time of publication of this report, Director of WES was Dr. Robert W. Whalin. WES Commander was COL Leonard G. Hassell, EN.

CONTENTS

	<u>Page</u>
PREFACE	1
LIST OF TABLES	3
LIST OF FIGURES	3
CONVERSION FACTORS, NON-SI TO SI UNITS OF MEASUREMENT	4
PART I: INTRODUCTION	5
Purpose	5
Armor Units, Concrete Armor, and Dolosse	5
Obstacles to Development of Comprehensive CAU Design Methods	10
CAU Structural Design Development History.	14
PART II: DOLOS DESIGN PROCEDURE	18
Overview	18
Preliminary Dolos Design	20
Intermediate Dolos Design.	36
Final Dolos Design	40
PART III: APPLICATION OF THE DESIGN METHODOLOGY.	42
General Design Diagrams	42
Application of Design Methods to Existing Dolos Structures	44
PART IV: SUMMARY AND CONCLUSIONS.	49
REFERENCES	50
APPENDIX A: CAUDAID: Concrete Armor Unit Design Aid	A1
Purpose.	A1
Background	A1
Program Description and Availability	A1
Program Layout	A2
Design Example	A5
APPENDIX B: NOTATION	B1

LIST OF TABLES

<u>No.</u>		<u>Page</u>
1	CAU Loadings	7
2	Comprehensive CAU Design History	14
3	Crescent City Prototype Dolos Study Tasks.	16
4	Dolos Static Distribution Moments.	25
5	Dolos Structures Throughout the World.	45
6	Design Stresses for Various Dolos Applications	47
A1	Screen 4 Horizontal Menu Item Descriptions	A3
A2	Screen 4 Vertical Menu Item Descriptions	A3

LIST OF FIGURES

<u>No.</u>		<u>Page</u>
1	Various concrete armor unit shapes	6
2	Dolos definition sketch	9
3	42-ton dolosse at Crescent City, CA.	11
4	CAU design methods and design requirements	12
5	Path required before dolos design	19
6	Preliminary dolos structural design.	21
7	Definition sketch for principal stress computation	22
8	Dolos waist ratio versus fractional stress	26
9	Dolos intermediate structural design	37
10	Dolos final design	40
11	Dolos stress versus weight	42
12	Dolos design diagram	43
13	Dolos design diagram with worldwide dolos applications	48
A1	Crescent City 1986 rehabilitation dolos design values as output from CAUDAID.	A5
A2	Dolos waist ratio versus stress coefficient as output from CAUDAID	A6
A3	Dolos size versus added stress per layer as output from CAUDAID.	A7
A4	Dolos design nomograph as output from CAUDAID.	A7
A5	Dolos combined exceedance probability function as output from CAUDAID.	A8

CONVERSION FACTORS, NON-SI TO SI
UNITS OF MEASUREMENT

Non-SI units of measurement in this report can be converted to SI units as follows:

<u>Multiply</u>	<u>By</u>	<u>To Obtain</u>
feet	0.3048	metres
inches	2.54	centimetres
pounds per square inch	6.895×10^{-3}	megapascals
pounds (mass) per cubic foot	16.01846	kilograms per cubic metre
tons (2,000 pounds, mass)	907.1847	kilograms

DOLOS DESIGN PROCEDURE BASED ON
CRESCENT CITY PROTOTYPE DATA

PART I: INTRODUCTION

Purpose

1. Concrete armor unit (CAU) structural failure has been a primary factor in the breakdown of many coastal rubble structures. Rational CAU structural design has been slow to develop due to the complex and random nature of the armor layer loads and the resulting response. CAU structural design is currently based on engineering judgement with little or no rigorous analysis. The CAU structural designer must have design methods that combine both deterministic and probabilistic techniques in order to develop both safe and cost-effective designs. The purpose of this report is to propose design methodologies for the safe design of dolosse and to provide a template for general CAU design.

Armor Units, Concrete Armor, and Dolosse

Engineering characteristics of armor

2. Armor units are used to protect coastal rubble-mound structures from erosion by the sea. Many types of armor unit shapes are available and each has its own engineering performance characteristics. The various categories of armor units include stone, concrete blocks, concrete mats, and slender complex-shaped concrete units. The default armor unit is stone for both economic and aesthetic reasons. CAUs are used when the costs associated with quarrying, transporting, and placing stone armor large enough to be hydrodynamically stable exceed those of CAUs. In high wave energy environments, such as the U.S. west coast and Pacific Ocean islands, concrete armor is often a design alternative because of the high costs of large stones. In lesser wave energy locations such as the U.S. east coast and along the Gulf of Mexico coastline, concrete armor will be increasingly important as stone armor availability decreases.

3. CAUs, as shown in Figure 1, come in a variety of shapes. While many different CAU shapes have been developed, CAU shapes fall somewhere

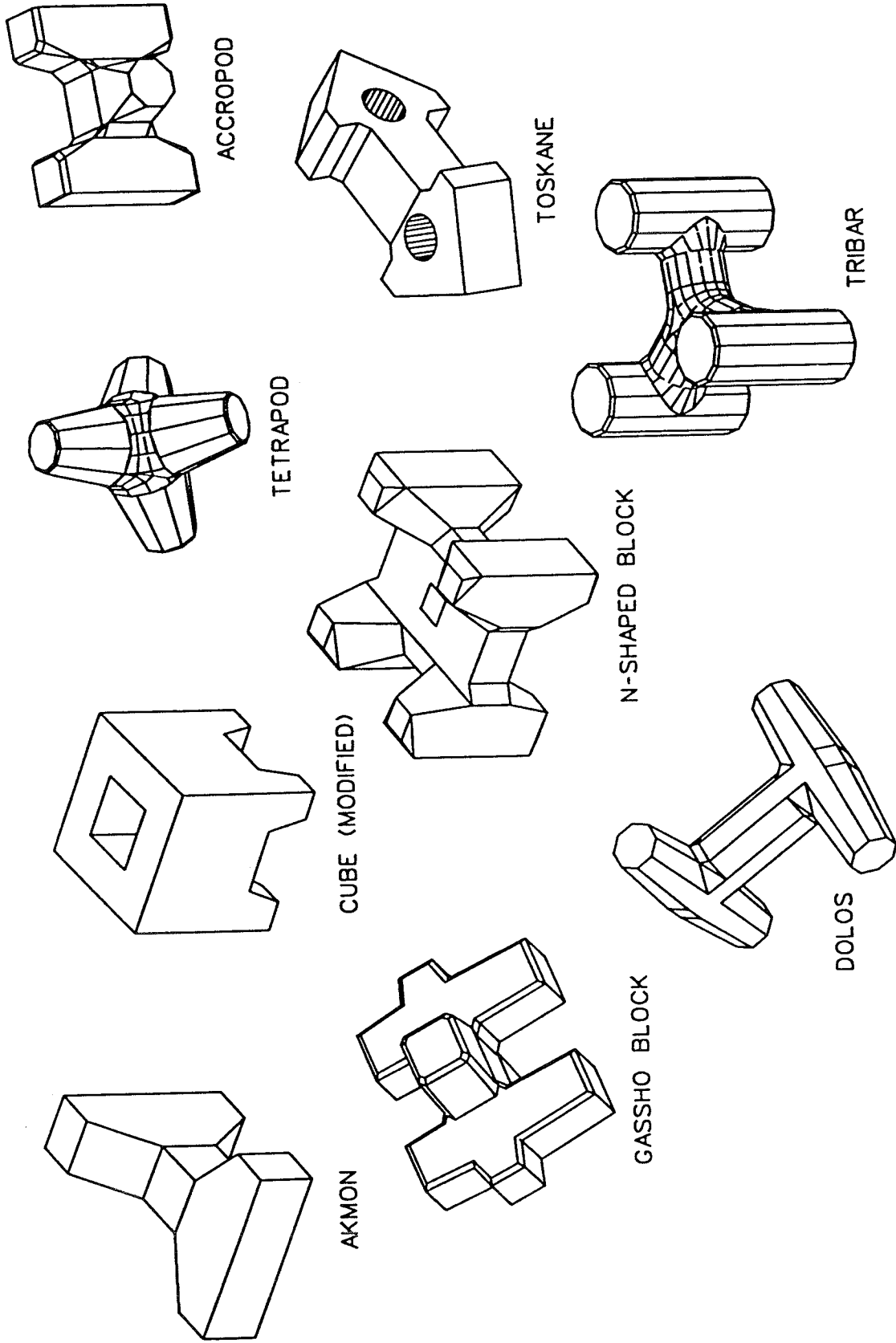


Figure 1. Various concrete armor unit shapes

between the two extremes of solid blocks and slender-legged units. Examples of very slender-legged units include the dolos and the tribar, while the tetrapod and accropode could be described as stout-legged units. Concrete armor can also be categorized according to the placement strategy: regular or random. The discussion in this report is restricted to randomly placed armor.

4. For stone armor, poor performance is generally due to hydrodynamic instability, with stones being dislodged by waves. Breakage of stone armor is not a problem if care is taken in choosing a quarry site and quarrying the stone. On the other hand, poor performance of concrete armor is due to combined hydrodynamic instability and armor breakage or severe abrasion. For CAUs, the breakage and abrasion can be a function of the units rocking, but need not be. The units can fail statically due to their own weight, or due to the weight of surrounding units, when subjected to unfavorable boundary conditions (Melby and Howell 1989). Concrete units can be abraded by unit-to-unit contact or by small sand particles and pebbles, entrained by highly turbulent breaking waves. Abrasion generally reduces the ability of the section to resist loads or reduces cover over steel-reinforced sections, accelerating corrosion of the steel.

5. Instability-induced impact loads generally result in accelerated breakage which produces more instability. Therefore, the armor unit-to-unit interlocking characteristics, which resist armor movement, are of primary importance to the performance of concrete armor. But increasing interlocking requires slender appendages, which are less able than stout appendages to resist forces due to self weight, adjacent units, waves, and rocking or projectile impacts. Thus, stout-legged units may produce less interlocking and hence, less residual stability, but they are also less susceptible to structural failure.

Table 1
CAU Loadings

<u>Load Category</u>	<u>Load</u>
Static	Self Weight
	Wedging
	Buoyancy
Dynamic	Pulsating
	Impact
	Abrasion
Material	Thermal
	Chemical

Tradeoffs between stout and slender armor

6. The perfect CAU shape would depend on the specific environmental conditions and would therefore be unique to each site. But development of armor units must be restricted to a few shape groups because of the high cost of developing general design guidance for the complex coastal structure environment. The optimal armor unit shapes will be hybrids between the strong stout units and the weaker, but hydrodynamically stable, slender units. Even restricting the CAU selection to a few select shapes, the choice of armor requires consideration of a great many complicated and inter-related factors.

7. Because stout armor units such as the accropode and modified block have no thin sections, sophisticated structural design methods are generally not required for these units. Stout CAUs require a steep slope to maintain stability because of the low degree of interlocking. And while these steep slopes are less expensive because they require less material than flatter slopes, they can fail in a very abrupt and catastrophic manner, should instability occur.

8. On the other hand, slender armor units, such as the dolos, tetrapod, and tribar can be built on either flat or steep slopes. But if the slender units fail structurally, a steep slope can promote abrupt failure. Excessive breakage of slender units on coastal structures worldwide simply shows that these units are not being designed with adequate strength or appropriate geometry. Therefore, in order to compare slender and stout units, one must assure that both will remain structurally intact. Holzhausen and Zwamborn (1991) showed that accropodes and dolosse have about the same stability on the steep slope of 1V:1.5H. They showed that dolosse have more reserve stability than the accropodes, provided they have enough strength in the slender appendages to resist static, wave-induced, and impact loads.

Why use dolosse?

9. As stated previously, the dolos armor unit (Merryfield and Zwamborn 1966), shown in Figure 2, is a good example of a slender armor unit because it exhibits very high hydrodynamic stability due to the interlocking slender flukes. But the slenderness of the dolos makes it susceptible to structural failure. The Sines breakwater failure, for example, is believed to be partly due to the structural failure of slender unreinforced dolosse (Baird et al. 1980).

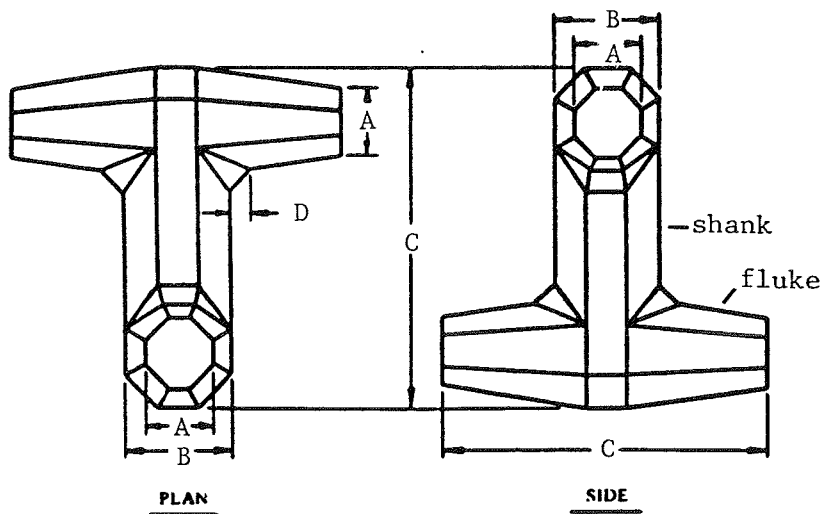


Figure 2. Dolos definition sketch

10. This structural fragility of the dolos can be managed through the careful use of a comprehensive design procedure that permits calculation of a design stress level. The dolos is unique in that analytical methods, as described in this report, can be used to optimize the shape for structural strength, depending on the given design conditions, without significantly affecting the hydrodynamic stability. Dolosse can therefore be safely used as long as the in-service structural response can be determined. The primary advantages of the dolos unit can be summarized as follows:

- a. High hydrodynamic stability and efficient wave energy dissipation.
- b. High porosity, reducing overtopping.
- c. Measurement of prototype structural response at Crescent City.
- d. Much experience with the unit, both in the lab and in the field.
- e. Ability to optimize shape for hydrodynamic and structural stability.
- f. Shape is conducive to small-scale structural instrumentation allowing measurement of design stresses in the laboratory.
- g. Ease in casting, storing, transporting, and placement.
- h. No members thick enough to produce thermal cracking during curing.

11. For the above reasons, the dolos armor unit should economically satisfy the armoring needs for many breakwater applications. Yet other CAU shapes, such as the accropode and the tetrapod, may be more efficient in certain circumstances. Although this report focuses on dolos design, it is not the intention of the author to promote dolosse as the only rubble-mound armoring solution. But the methods discussed herein provide a framework for both designing slender concrete armor and comparing competing armor shapes.

Obstacles to Development of Comprehensive CAU Design Methods

12. After several breakwaters sustained massive and unexpected armor unit breakage and subsequent armor layer unraveling during the 1960's and 1970's, new techniques for CAU hydrodynamic and structural design began appearing in the literature. But comprehensive CAU design methodologies have been slow to develop because of three primary factors:

- a. The multitude of different armor unit shapes spreads design development efforts too thin.
- b. The structural and hydrodynamic physics are complex.
- c. The CAU design problem is unlike both typical coastal rubble-mound design and conventional structure design.

The following paragraphs discuss these items individually.

Too many CAU shapes

13. The CAU engineering problem is so complex that formulation of a viable design solution requires international research coordination, both for technical reasons and because of funding limitations. But the large number of different CAU shapes in use has limited worldwide research coordination, resulting in sporadic progress in concrete armor unit design technology. The fact that many of the armor unit shapes are proprietary has also restricted coordinated research. Recent coordinated research concerning the dolos unit, as described in this report, has resulted in the development of advanced design methods.

Complex physics

14. The physics of the CAU design problem are complex in several respects. First, the very nearshore waves and the highly turbulent breaking or broken wave, as it flows into and runs up the face of a breakwater, are not presently analytically solvable. Second, the randomly placed armor units

present random boundary conditions and highly varying drag profiles (Figure 3). Finally, the CAUs are generally unreinforced and because of their deep sections and irregular shape, the stress-strain behavior of the concrete is difficult to predict. Therefore, the design methods for any one CAU shape must be unlike any other coastal or land-based method.

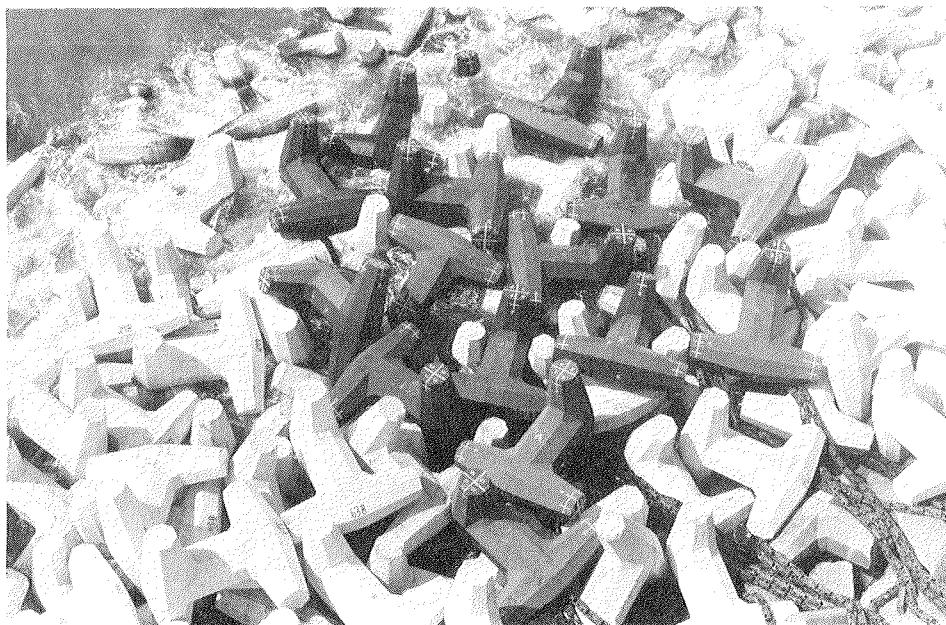


Figure 3. 42-ton dolosse at Crescent City, CA

CAU design unlike any other

15. Until recently, no general CAU structural engineering design tools were available. CAU design has been limited to determining the hydrodynamic stability using empirical formulae like the formulae developed by Hudson (1958) and more recently by van der Meer and Pilarczyk (1987). The hydrodynamic stability design formulae generally assume that the critical design condition occurs when several armor units are displaced from their equilibrium positions, exposing the underlayer to direct wave action. The hydrodynamically stable weight determined from an empirical formula is typically verified in a physical model.

16. In a conventional hydrodynamic stability model study, the strength of the armor units is not scaled. The units are made of grout or polyester materials, which produce model strengths several orders of magnitude greater than scale. Thus, traditional design methods assume that the armor units will remain structurally intact. But experience has shown that a breakwater might

still unravel and ultimately fail due to structural failure of several CAUs even though model tests showed a stable armor layer. Thus traditional CAU design methods based solely on hydrodynamic stability are inadequate.

17. Figure 4 shows CAU design methods, which include structural response determination as suggested by various researchers. Also shown in this figure are the armor layer design requirements. The table shows which design requirements are satisfied by a particular design methodology. It is evident that the only design methods satisfying all of the design requirements are the stochastic stress methods as proposed herein. The following paragraphs describe the pros and cons of each of the design methods.

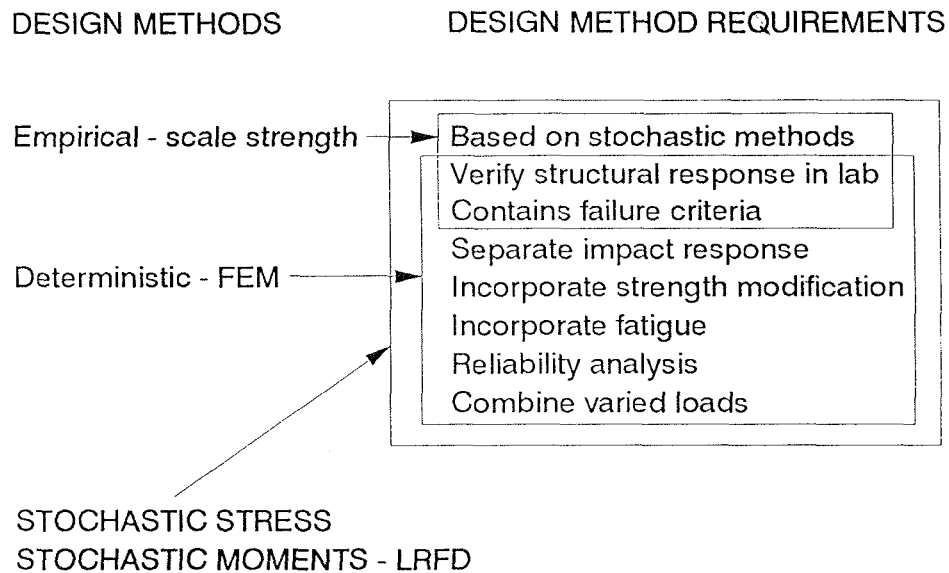


Figure 4. CAU design methods and design requirements

Empirical CAU design methods

18. Determining an armor unit structural failure empirical formula and verifying structural failure in the small-scale physical model simultaneously with hydrodynamic stability would be advantageous because, as noted above, the CAU structural strength and hydrodynamic stability are coupled. Empirical methods have been developed to determine the structural response of armor units in conjunction with small-scale model stability tests. Timco and Mansard (1982) were successful in developing scaling criteria for the structural failure of concrete armor units. This methodology is very attractive from a design point of view, but application of the method is expensive and

difficult. The primary technical problem with the method is that there is no way to separate the response due to the different forcing functions. The unit-to-unit impact loads scale differently than do the wave and self-weight loads. To scale the entire response requires a material that is too difficult to work with in the laboratory.

Conventional structural analysis methods

19. Seawall design is similar to conventional land-based structural design where conventional structural analysis techniques are used with lab and field-measured loadings to determine the internal stresses and overturning moments. This is the classical approach to structural analysis where the loads are determined and then applied to the structure, and analytical and numerical methods are used to solve for the structural response. In conventional structural design, load factors are often applied to the loads to account for understrength or overload. The structural response to these modified loads is commonly analyzed using deterministic matrix methods such as a stiffness formulation or, for continuous media, finite element methods (FEM). The individual members are sized to resist the maximum stresses.

20. But conventional structural analysis cannot be employed for armor layer analysis because the loadings are not yet known. Many laboratory tests with the appropriate instrumentation would be required to quantify the loads on a given armor unit for any given set of design parameters. Even then, because the boundary condition scenarios are so varied and the concrete behavior difficult to quantify, accurate stress quantification by a design engineer would be technically very difficult and not economically feasible.

Stochastic stress design methods

21. The design method discussed in this report follows basic reliability techniques with determination of the armor layer design stress from a design probability distribution of maximum design stresses. Using this stochastically based design method, the designer need not be concerned with the loads on, or the stresses within, each design stress. This design procedure utilizes deterministic modifications to prototype design static and pulsating stress distribution statistical moments to compute separate design distributions. Handling the static and pulsating stress distributions separately allows independent modification and scaling of the distributions. The individual distributions are computed and combined in the microcomputer-based program called CAUDAID (Concrete Armor Unit Design Aid) (Appendix A).

The dolos design can be optimized with respect to dolos shape, size, and material characteristics within the computer program.

22. This design methodology also includes design stress and hydrodynamic stability verification in the physical model. Thus, all of the primary design requirements are met under this design procedure.

CAU Structural Design Development History

23. Major progress toward a complete CAU design procedure was not achieved until very recently. Table 2 shows the history of recent CAU design methods. Note that all of the innovations occurred since 1980. The most significant milestones in CAU design development are shown in bold lettering in this table.

Table 2
Comprehensive CAU Design History

<u>Authors</u>	<u>Date</u>	<u>Development</u>
Burcharth	1981	Identified load types
Burcharth	1981	Prototype drop tests
DHI	1981	Instrumented small-scale CAU units
Timco and Mansard	1982	Scaled CAU strength
Howell, ed.	1985	Two moments and a torque
Scott et al.	1986	Load cell
McDougal, Melby, and Tedesco	1987	Dolos numerical model
Howell et al.	1988	Prototype dolos measurements
Melby	1989	Dolos design procedure
Howell, Rhee, and Rosati	1990	Pulsating distribution model
Markle and Greer	1990	Verified load cell for pulsating
Burcharth and Liu	1990	Verified load cell for static
Burcharth and Melby	Current	Parametric dolos study

24. Progress toward a comprehensive CAU design procedure began in earnest in the late 1970's and early 1980's. Burcharth (1981) identified the primary CAU load types (Table 1) and proposed prototype drop tests to determine general dolos failure. The Danish Hydraulic Institute experimented

with externally strain-gaged armor during this same time period. Timco and Mansard developed their strength scaling relation during this period as described previously.

25. The Crescent City Prototype Dolos Study Workshop (Howell 1985) was instrumental in setting the stage for the bulk of the current CAU design philosophy. At the workshop, the concept of characterizing the structural response of a dolos as two moments and a torque was introduced. It was the consensus of the attendees at the workshop that these parameters would be measured at the shank-fluke interface, where stress concentrations cause the highest stresses. Also, due to the random boundary conditions and wedging forces in the armor layer, it is impossible to develop an unambiguous relationship between the stresses at mid-shank and the stresses at the shank-fluke interface. So mid-shank instrumentation could not be used to determine the maximum stress at the shank-fluke interface.

26. Also at the workshop, McDougal and Tedesco showed initial results from an FEM numerical model for prediction of the stresses in a single dolos. This work was later extended to include a wave force numerical model and a rigid body stability model (McDougal, Melby, and Tedesco 1987). These numerical approaches based on wave force models relied on semi-empirical deterministic wave-force-on-cylinder equations with deterministic boundary conditions.

Crescent City Prototype Dolos Study

27. Following the 1985 workshop, a detailed plan was formulated for the Crescent City Prototype Dolos Study. The Crescent City study was broken down into individual tasks, each carefully designed to produce products that would feed into the dolos design procedure and mesh with the other study products. The tasks are listed in Table 3. Other than the design procedure development, the tasks are divided into three groups: (a) prototype data collection, (b) physical model tool verification, and (c) deterministic dolos analyses.

28. The data collection task included collection of free surface elevation, dolos strains from 14 instrumented dolosse, photographic records of the breakwater and instrumented dolosse, and pressure signals from pressure gage arrays inside the breakwater and just off the breakwater toe. The deterministic tasks consisted of analyses using primarily FEM models. The results of all of the tasks were used in the design procedure development.

Table 3
Crescent City Prototype Dolos Study Tasks

Task Area	Task	Description
Prototype data collection	Data collection	Collect prototype dolos strain and wave data
	Movement	Quantify both short and long-term dolos movement
	Boundary conditions	Create database of boundary conditions of instrumented dolosse
Physical model tool verification	Physical model	Construct and validate load cell
Deterministic dolos analyses	Impact	Quantify impact response
	Waist ratio	Determine effect of changing waist ratio on stress
	Stacking	Determine effect of dolos stacking depth on stress
	Critical size	Determine critical dolos size
	Fatigue	Determine fatigue in dolosse
	Reinforcement	Determine reinforcement requirements in dolosse
Design development	Design procedure	Create dolos design procedure

29. Possibly the most significant event in CAU design development was the acquisition of prototype dolos structural response data at Crescent City (Howell 1988). The prototype data provided several startling revelations, the most significant of which was the magnitude of the static stress levels, both absolute and relative, to pulsating response (Melby and Howell 1989). Previous FEM studies showed insignificant static stress levels for all but the most unfavorable boundary condition scenarios. So prototype static stress levels ranging from 100 psi* to 900 psi with a mean of 416 psi and a standard

* A table of factors for converting non-SI units of measurement to SI units is presented on page 4.

deviation of 188 psi were astounding. The difference between FEM static stresses and prototype data is thought to be due to the wedging loads resulting from the binding effect of the nesting armor layer. The prototype data also showed the maximum pulsating stress to be surprisingly well-behaved and highly correlated with the average of the highest one-tenth of the waves ($H_{1/10}$) (Howell, Rhee, and Rosati 1990). Additionally, the prototype data revealed that the dolos static stress was increasing over time at a rate of approximately 26 psi per year (Melby and Howell 1989, Kendall and Melby 1992).

30. While the Crescent City prototype data yielded considerable insight into the dolos structural response, it was also used in the physical model dolos instrumentation verification. Markle (1990a) showed that small-scale dolosse embedded with the load cell could be used to measure pulsating stresses in the physical model that could be correctly scaled to prototype. Thus, structural measurements could be done simultaneously with hydrodynamic stability studies. Burcharth and Liu (1990) later showed that the load cell could also be used to measure scalable static response in the physical model, provided the dolos surface friction was correctly scaled. The load cell has not been calibrated for impact response. Because the material elasticity scaling is difficult with the load cell, accurate measurement of impact response in the small-scale model using this instrument requires more research.

31. As stated earlier, the Crescent City prototype data were augmented by deterministic results from FEM studies to arrive at the dolos design procedure as presented herein (Melby and Howell 1989). This design procedure utilizes FEM results to modify scaled prototype stress distributions. Static and pulsating stress distributions are modified for waist ratio, stacking depth, material unit weight, and dolos size. The modified distributions are combined to achieve a design stress distribution. So, given a design stress probability, the designer can determine a design stress level for the armor layer. The design stress is compared to a fatigue-reduced strength to give a factor of safety. All of these calculations are incorporated into the micro-computer program CAUDAID.

PART II: DOLOS DESIGN PROCEDURE

Overview

32. Of the loads listed in Table 1, the three primary loading mechanisms are static, pulsating, and impact. But the structural designer requires an overall maximum design stress. Because the boundary conditions and the loadings are random, this design stress must be based on a single design probability function. This probability function will be some combination of the static, pulsating, and impact response principal stress probability distributions.

33. It has been shown by Melby and Howell (1989) and Melby, Rosson, and Tedesco (1990) that the static stresses measured in the Crescent City dolosse were close to the critical strength of the concrete. Because of these high stresses in large slender armor units, there is little residual strength in the units to resist pulsating and impact loads. Pulsating loads have been shown to be small relative to static loads and would therefore not be expected to affect the design stress significantly. But impact loads due to dolos rocking and projectiles in the armor layer could be large and the large slender unreinforced dolosse do not have the capacity to resist these loads. This design procedure is therefore focussed on the probabilistic combination of static and pulsating stresses only, for the design of large dolosse. Future revisions will incorporate the impact response to facilitate the strength design for smaller and/or reinforced dolosse.

34. Some probability distributions used in this report are based on the normal distribution.

$$p(x) = \frac{1}{\sqrt{2\pi s}} \exp \left[-\frac{1}{2} \left(\frac{x - \mu}{s} \right)^2 \right] \quad (1)$$

The manipulation and combination of these distributions can be mathematically laborious but can be done quite easily numerically. Thus, the microcomputer program CAUDAID has been developed to automate the manipulations of the probability distributions. This report provides a detailed discussion of the analytical methods and assumptions underlying the CAUDAID algorithms. Appendix A provides a discussion of the program CAUDAID and gives a design example showing program input and output.

35. The Crescent City Dolos Structural Design Procedure is divided into three phases: (a) Preliminary Design, (b) Intermediate Design, and (c) Final Design. These modules, or design phases, are subsets of the breakwater modular design procedure. The first phase, the preliminary or reconnaissance design phase, is a desktop study that utilizes the program CAUDAID to determine a dolos design configuration. The second phase utilizes the physical model, if necessary, to verify both the design stress level and the hydrodynamic stability of the design dolos. The final phase includes evaluation of the design stress and, if necessary, evaluation of special strengthening schemes.

36. The path required prior to entering the dolos structural design procedure is shown in Figure 5. It includes evaluation of the project goals

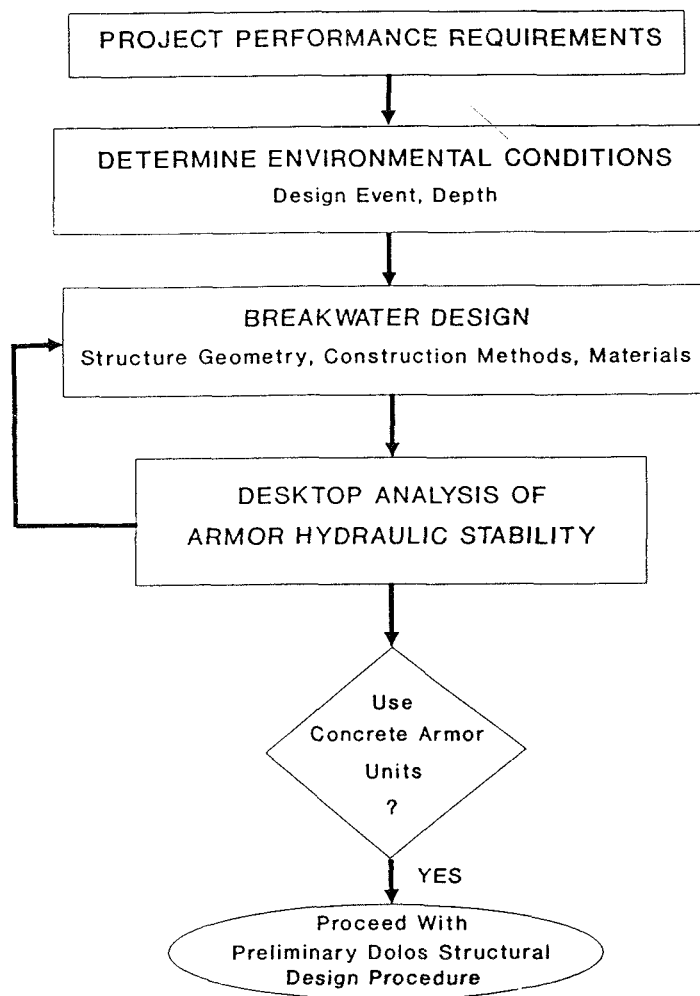


Figure 5. Path required before dolos design

and the general site conditions to narrow the selection of structure possibilities. In the first stages of breakwater design, the environmental design parameters are determined. These include design wave characteristics and site bathymetry. The next step generally is to determine the structure geometry, including profile and cross-sectional layout. Alternative armor unit sizes, shapes, and material characteristics can be judiciously selected to optimize the hydrodynamic stability for the given structure. If CAUs are chosen over stone, then the preliminary dolos design procedure will be initiated.

Preliminary Dolos Design

37. Parameterizing the dolos structural response as a maximum principal tensile stress occurring at a critical cross section has the following advantages over other methods.

- a. Allows reduction of the complex stress state within the armor layer matrix to a single stress design distribution.
- b. Allows reduction of several gross structural measurements, such as the two moments and a torque measured in the prototype and in the physical model, to one stress parameter.
- c. Allows scaling of the response to different loadings separately and allows the combination of the separate response probability distributions.
- d. Allows coupling of hydrodynamic stability with strength design and allows shape optimization and strength enhancement using analytical tools.
- e. Permits comparison of structural response with structural failure criteria.
- f. Expedites the mechanics of the design process using a microcomputer-based program.

Determining the design principal stress in this manner requires some assumptions, as discussed below, and can only provide an approximation to the actual stress state (Melby, Rosson, and Tedesco 1990). Yet the probability distributions generated from these approximate stresses appear to define the extreme (design) stress states well. The primary disadvantage to using a single stress parameter is that conventional reinforcement analyses for flexure and torsion cannot be done efficiently. Methods for reinforcement analysis are being finalized and will be published in the near future.

38. As illustrated in Figure 6, the individual principal stresses for a given structure can be expressed as exceedance probability functions (EPFs). The preliminary principal stress joint EPF can be determined by combining the individual EPFs from the static, pulsating, and impact responses. This requires that the individual responses be independent. There is negligible error in this assumption because the static response is independent from the pulsating and impact responses. The question of independence of pulsating and impact response is not addressed because, within this design procedure, only the combination of static and pulsating stress distributions is given, for reasons discussed in the previous section.

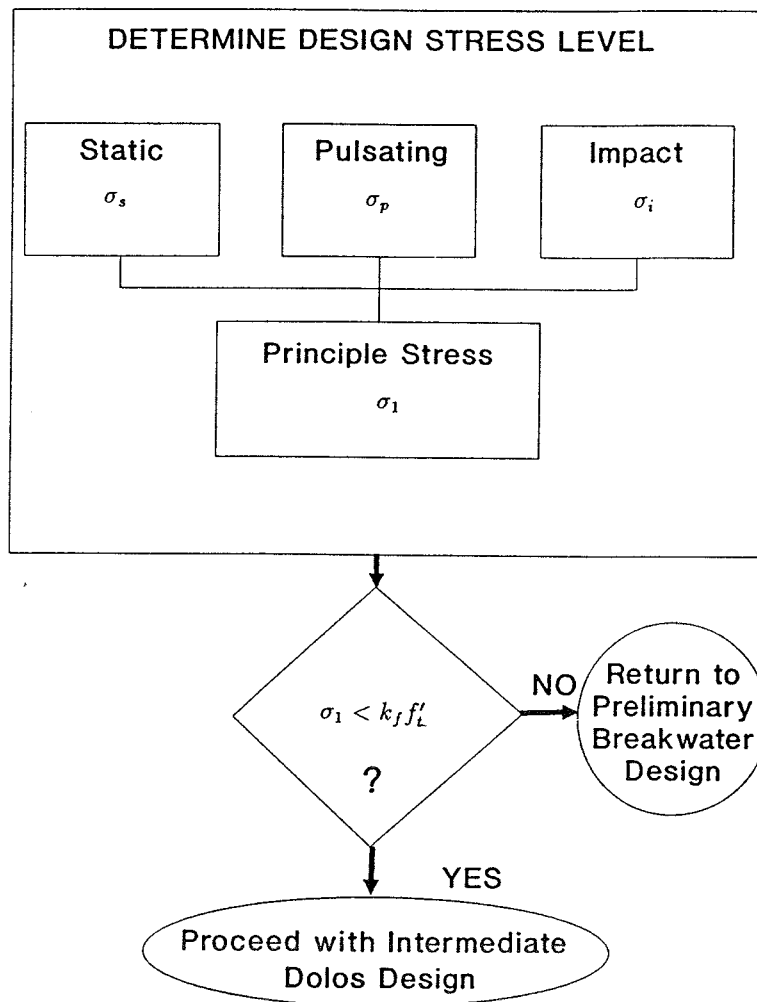


Figure 6. Preliminary dolos structural design

Computation of Principal Stress

39. The measured moments and axial load can be combined into a single uniaxial stress component using a combined biaxial bending and axial formula

$$\sigma_{zz} = \frac{M_x y}{I_x} + \frac{M_y x}{I_y} + \frac{P}{A} \quad (2)$$

where

M_x , M_y = moment about the x and y axes, respectively

x, y = distance along the x and y axes, respectively, from the neutral surface to the point of measurement

I_x , I_y = moments of inertia

P = axial load

A = cross-sectional area

Note that in Figure 8 the moments M_x and M_y are also designated M_h and M_v , respectively. The h and v subscripts refer to horizontal and vertical moments and have been used in several Crescent City dolos references.

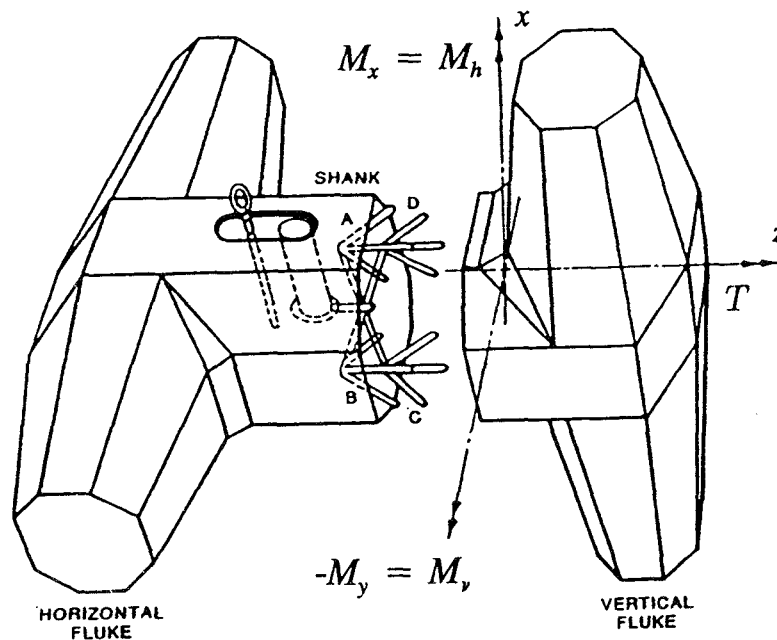


Figure 7. Definition sketch for principal stress computation

40. The maximum bending stress for the cross section can be found using an iterative technique by sampling the stress around the cross-section perimeter. In the prototype, axial strains were measured by summing rather than differencing the opposing strain gage bridges, but shearing strains due to flexure were not measured.

41. The derivation of Equation 2 assumes that plane sections remain plane during bending and that the material obeys Hooke's law (stress is proportional to strain). This relation therefore assumes a linear stress distribution across the section. While the FEM model has shown the stress distribution to be nonlinear, it appears that this analysis method provides a reasonable approximation of the maximum principal stresses; but further verification of this hypothesis is necessary (Melby, Rosson, and Tedesco 1990). Also, because the flexural shearing strains, and therefore stresses, are generally maximum at the section center and decrease to near zero at the outer fibers, they have been neglected in this measurement and analysis scheme. Although the FEM results above show this assumption to be invalid, Burcharth and Liu (1990) have shown this to be a reasonable assumption for the extreme stress states in which the designer is interested. Here also, further research is necessary.

42. The torque is combined with the bending stress to yield the planar principal stresses for an element at the outer surface as given below.

$$\sigma_1, \sigma_2 = \frac{\sigma_{zz}}{2} \pm \sqrt{\frac{(\sigma_{zz})^2}{2} + \tau^2}$$

43. The torsional shear stress τ is given by

$$\tau = \frac{Tr}{J}$$

where

T = torque

r = radius of the member

J = polar moment of inertia

Although these relations are derived for a circular cross section, they appear to be reasonably accurate if one assumes an effective diameter for the octagonal dolos cross section. The preceding assumptions indicate that this principal stress is an approximation to the actual stress state within the dolosse.

44. Melby, Rosson, and Tedesco (1990) also showed that, although axial stresses are in general compressive, they can be tensile and add significantly to the maximum tensile stress. It was shown that two prototype dolosse had

tensile axial stresses that increased the principal static stress by 17 percent and 34 percent. From results of large-scale tests, Burcharth and Liu (1990) have shown that dolos axial stresses are relatively small for extreme stress states. It is also likely that the axial stresses will not significantly affect the static stress probability distributions that will be used to determine the design stress level. The maximum prototype stresses without axial contributions are therefore reasonable estimates of likely maximum static stresses on the breakwater.

Static response

45. In general, the static dolos stress can be computed as the mean of a given stress time series. The stress time series is computed as shown in the previous section. Of course, the mean of the time series may not be the static stress if the oscillations in the time series are not symmetric about the mean or if there is drifting or shifts in the data set. These peculiarities in the data set must be accounted for in the computation of the mean. For the Crescent City prototype data, there were few shifts and little drifting in the 30-min time series and nearly all of the data were symmetric about the mean so the static response was computed as the mean of the time series in all cases.

46. Although the static data set for the Crescent City prototype dolosse is a very small sample consisting of the 14 maximum stress values corresponding to the 14 working instrumented prototype dolosse, a conservative probability density function (PDF) can be fit to this data set. For the histogram, the mean is $m_{cc} = 416$ psi and the standard deviation is $s_{cc} = 188$ psi, where the subscript cc indicates that the moments were determined using Crescent City prototype dolosse data. The best-fit PDF to the static stress histogram is of the log-normal type and can be characterized as

$$P(\sigma_{scc}) = \frac{1}{\sigma_{scc}\beta_{cc}\sqrt{2\pi}} \exp \left[-\frac{1}{2} \left(\frac{\ln \sigma_{scc} - \alpha_{cc}}{\beta_{cc}} \right)^2 \right] \quad (3)$$

where the mean of $\ln \sigma_{scc}$ is given by $\alpha_{cc} = 5.93$, and the standard deviation is given by $\beta_{cc} = 0.45$. Due to the extremely small data set, the fitting of the density function was done visually. The log-normal distribution represents the skewness and the tail or extremal values of the data well. Also, Burcharth and Liu (1990) support this distribution for static dolos response with large-scale test results. The static stress can be nondimensionalized by

the product of the unit weight and the dolos fluke length or

$$\sigma'_s = \frac{\sigma_s}{\gamma C} \quad (4)$$

Nondimensionalizing the stress by γC permits scaling of the stress for both unit weight and dolos size. The nondimensional mean and standard deviation for Crescent City dolos static response are given in Table 4 along with the dimensional values. Variables in this table subscripted with 'cc' are calculated directly from Crescent City dolos data, while those variables without the subscript are for the design dolos.

Table 4
Dolos Static Distribution Moments

<u>Distribution</u>	<u>Static Stress Variable</u>	<u>Mean</u>	<u>Standard Deviation</u>
Dimensional histogram	σ_{scc}	$m_{cc} = 416$	$S_{cc} = 188$
Nondimensional histogram	σ'_{scc}	$m'_{cc} = 25.8$	$S'_{cc} = 11.7$
Nondimensional log-normal	$\ln\sigma'_{scc}$	$\alpha'_{cc} = 3.15$	$\beta'_{cc} = 0.45$
Modified log-normal	$\ln\sigma'_s$	α''	β''

47. The mean of the nondimensional prototype static stress distribution appears to be approximately double that of preliminary results of laboratory dolos static response tests. This difference between lab and prototype static stress results likely lies in the difference in slope. The instrumented prototype dolosse lie on a nearly flat slope. Visual inspection of the prototype dolosse shows that they have longer span lengths between boundary conditions than do the dolosse on steeper slopes, thus supporting this hypothesis. The prototype static stress statistics are therefore conservative.

48. One method of generalizing the nondimensional Crescent City static stress distribution given in Equation 3 is to simply apply scaling factors to the distribution moments. As part of the Crescent City prototype study, FEM stress modification studies were done for the dolos waist ratio, $r = B/C$, or the ratio of the width of the shank to the length of the fluke (Figure 2) and for the number of layers N_L of dolosse on the slope. These studies are

discussed in detail by Howell et al. (1992). The waist ratio results, shown in Figure 8, can be summarized with a quadratic fit of the fractional change in stress as a function of waist ratio as follows:

$$k_r = a_1 + a_2 r + a_3 r^2 + a_4 r^3 \quad (5)$$

where $a_1 = 5.139$, $a_2 = -28.738$, $a_3 = 66.071$, and $a_4 = -52.083$.

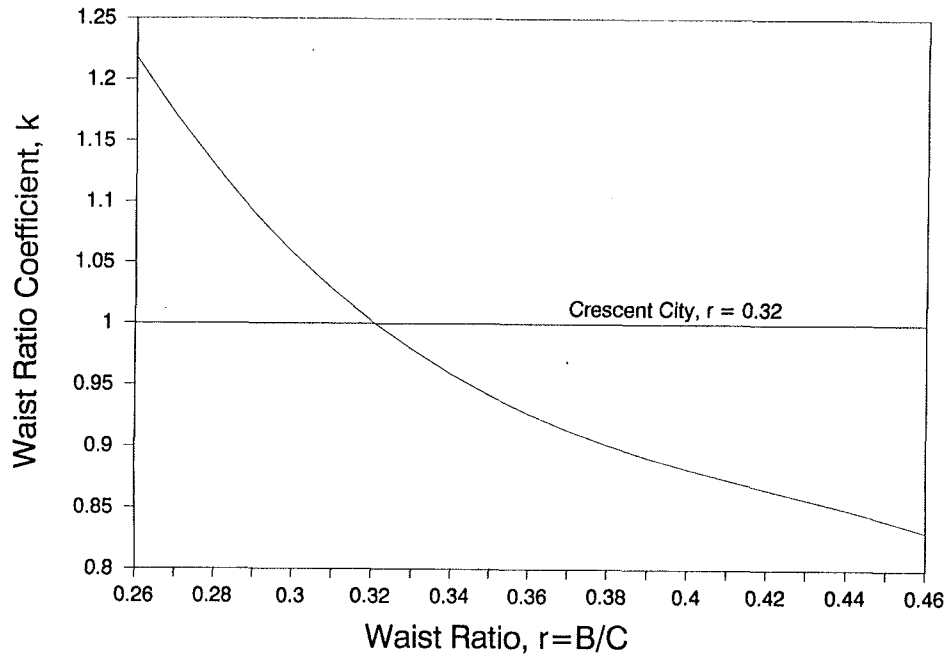


Figure 8. Dolos waist ratio versus fractional stress

49. The layer modification can be thought of as a constant shift in the stress for each layer added. This shift can be represented by the following formula:

$$\sigma_{sL} = \frac{S_L C}{\gamma C} (N_L - 1) \quad (6)$$

where

σ_{sL} = the nondimensional increase in stress per added layer

S_L = 0.53 psi/in., the dimensional layer coefficient

N_L = the total number of layers

Note that S_L assumes that C is in inches and γ is in pounds per cubic inch. Equation 6 assumes that the maximum static stress will be in the lowest layer.

50. The Crescent City static PDF can now be generalized using these two stress modification relationships. The generalized nondimensional random stress variable for the static stress distribution can be expressed as

$$\sigma'_s = k_r \left(\frac{\sigma_s}{\gamma C} \right)_{cc} - k_{rL} \left(\frac{S_L C}{\gamma C} \right)_{cc} + k_{rL} \left[\frac{S_L C}{\gamma C} (N_L - 1) \right] \quad (7)$$

where k_r and k_{rL} are the waist ratio modification factors. The additional waist ratio modification factor, k_{rL} , is required because k_r does not include the effect of added layer stress with changing waist ratio. The added stress per layer should decrease as the waist ratio increases due to the decrease in unsupported length. In Equation 7, the first term is the nondimensional Crescent City static stress modified for the design waist ratio, the second term is the reduction in stress due to removal of the second layer of dolosse, and the third term is the increase in stress due to the added layers of the design dolos. Note that the subscript cc on the first and second terms indicates that all of the variables in that term are for the Crescent City dolosse. The third term variables are those of the new design dolos.

51. Assuming that

$$k_{rL} \approx k_r \quad (8)$$

Equation 7 becomes

$$\sigma'_s = k_r \left[\left(\frac{\sigma_s}{\gamma C} \right)_{cc} + S_L \left(\frac{1}{\gamma} (N_L - 1) - \frac{1}{\gamma_{cc}} \right) \right] \quad (9)$$

which can be reduced to

$$\sigma'_s = k_r (\sigma'_{scc} + a) \quad (10)$$

where the shift parameter is given by

$$a = S_L \left[\frac{1}{\gamma} (N_L - 1) - \frac{1}{\gamma_{cc}} \right] \quad (11)$$

52. Now the design static distribution in terms of the generalized random variable given in Equation 10 is

$$p(\sigma'_s) = \frac{1}{\sigma'_s \beta'' \sqrt{2\pi}} \exp \left[-\frac{1}{2} \left(\frac{\ln \sigma'_s - \alpha''}{\beta''} \right)^2 \right] \quad (12)$$

and the mean and standard deviation for this log-normal distribution are

$$\alpha'' = \text{mean} (\ln \sigma'_s) \quad (13)$$

$$= \ln[k_r(m'_{cc} + a)] - \frac{1}{2} (\beta'')^2 \quad (14)$$

and

$$\beta'' = \text{s.d.} (\ln \sigma'_s) \quad (15)$$

$$= \sqrt{\ln \left(\frac{s'_{cc}}{m'_{cc} + a} \right) + 1} \quad (16)$$

respectively. In the above equation, the mean of the nondimensional Crescent City static stress distribution is $m'_{cc} = 25.8$ and the standard deviation is $s'_c = 11.7$, as given in Table 4. Note that these values are not natural logs and are not moments of the log-normal distribution. They are computed directly from the data and are used to estimate the log-normal moments.

53. The above analysis assumes that the static response is not significantly affected by the armor layer porosity or slope. This assumption has not been validated and must be kept in mind when using the algorithms contained herein.

Long-term static response

54. Kendall and Melby (1990) showed, using prototype static data through 1989, that the Crescent City static stresses were increasing with time, at a decreasing rate. The exponentially decaying characteristic shape of this long-term time series and the fact that the stress increases were between 0 and 5 percent could have been attributed to creep in the concrete. But continued long-term monitoring of the Crescent City dolosse has shown the static stresses to be increasing linearly rather than increasing with an exponential decay (Coastal Engineering Research Center 1992, Kendall and Melby

1992). Thus the static stress increase is probably due more to the continued nesting of the dolos armor layer.

55. The static stress distribution given in Equation 3 includes the measured maximum static stresses in each of the instrumented Crescent City dolosse during the period from post-construction in February 1987 to July 1990. So the long-term increase in static stress during this period is included in the distribution. Because it is not known if the mean static stress increase is approaching an equilibrium value, no explicit modification for long-term changes in stress is included in this design procedure. The stresses in the prototype dolosse continue to be monitored yearly and an adjustment factor for the time rate of change of stress will be incorporated in Equation 10 if the stresses continue to increase.

Tidal influences

56. Melby and Howell (1989) showed preliminary results from correlation analyses of sporadic static dolos moments versus tidal time series. The low correlation coefficients from this analysis were inconclusive, although the plots of tidal height and moments versus time indicated that the dolos static moments were correlated with tide. The tidal response of a dolos that is alternately dry and submerged is due to the reduction in self weight; the submerged weight of a dolos with a specific gravity of $S = 2.42$ is only 59 percent of the dry weight. The response of dolosse at or below the still-water level to fluctuations in tidal height is therefore obvious. But the Crescent City results apparently showed moment-versus-tide correlation for dolosse that were high and dry, above the still-water level. More recent data from the Crescent City dolosse have shown that this dry dolos quasistatic response is not due to tidal fluctuations but is caused by concrete shrinkage and swelling due to temperature variations throughout the day. This type of straining does not induce stresses in the dolosse and is therefore not a concern.

Pulsating response

57. The maximum pulsating stress is a function of the design wave height H , the exceedance probability E , and a wave stress constant k_{ps} (Howell, Rhee, and Rosati 1990). The Rayleigh distribution, given in Equation 17, best describes the Crescent City dolos pulsating response.

$$p(\sigma_p) = \frac{\pi \sigma}{\sigma_{pmax}^2} \exp \left[-\frac{\pi}{4} \left(\frac{\sigma}{\sigma_{pmax}} \right)^2 \right] \quad (17)$$

The mean of the maximum pulsating stress, which is linearly related to the average of the highest one-tenth ($H_{1/10}$) of the waves in a 30-min time series, can be expressed as

$$\bar{\sigma}_{pmax} = k_{ps} H_{1/10} \quad (18)$$

where

$$k_{ps} = 1.547 \text{ psi/ft} \quad (19)$$

where wave height is in feet. $H_{1/10}$ is computed using the zero-downcrossing method of analysis.

58. For dolosse at Crescent City, the pulsating response is very well defined. Because the mean of the maximum stresses for each 30-min time series is linearly related to $H_{1/10}$, the designer is able to choose a mean stress given the design wave height. This mean stress can then be used to generate a Rayleigh EPF. Other extremal probability distributions that can be used to model the pulsating response have been investigated, but the Rayleigh distribution has proved to fit the Crescent City data well at stress levels for which the designer is interested. The wave stress constant can be non-dimensionalized with dolos size and concrete density but is most likely site-dependent. As more pulsating response data become available from ongoing parametric physical model tests, the range of this constant will become better defined.

59. The random pulsating stress variable given in Equation 18 can be nondimensionalized as was done for static stress.

$$\bar{\sigma}'_{pmax} = \frac{k_{ps} H_{1/10}}{\gamma C} \quad (20)$$

60. Some variables that may affect this pulsating distribution but that are not explicitly included in this design procedure include:

- a. Effect of depth-dependent breaker shape on structural response.
- b. Shape of the wave spectrum.

- c. Wave directionality.
- d. Wave grouping.
- e. Dolos position on breakwater and in armor layer.
- f. Structure slope.
- g. Structure porosity.

The range of values of design interest for the first five items listed above for the Crescent City case are contained implicitly in the pulsating design distribution. For general application of this design procedure, although all of the variables listed above may have a significant effect on the dolos hydraulic stability, it is likely that they will not significantly affect the design stress distribution that is based solely on the combination of static and pulsating responses because the pulsating response is small compared to the static response. Therefore, exclusion of these variables is reasonable.

Impact response

61. Wave-induced impact. The impact stress is a function of the armor unit hydrodynamic stability. There will be no impacts below the stability threshold, but the impact stress above this threshold can be very high. Preliminary tests have shown the design impact stresses to be on the order of twice the combined static and pulsating stress for rocking in place. Because no impacts were observed in the Crescent City prototype dolos data, the design impact stress could not be determined for this initial design procedure. But because the prototype dolos static stresses approached the critical material strength, armor unit impact loads will not be allowed in the large dolos designs. The design procedure is configured such that impact response EPFs can be easily added in the future as they become available.

62. Construction-caused impact. For the reasons stated above, construction-caused impacts during dolos transport and placement must be minimized. Dolos placement from floating barge-mounted cranes should therefore be avoided.

Combined response

63. Given two independent PDFs, $f_x(x)$ and $f_y(y)$, the joint PDF can be written using the convolution integral as

$$f_z = \int_{-\infty}^{\infty} f_x(x) f_y(z-x) dx \quad (21)$$

and since

$$f_x(x) = 0 \quad x < 0 \quad (22)$$

and

$$f_y(z - x) = 0 \quad (z - x) < 0 \quad (23)$$

the convolution integral becomes

$$f_z = \int_0^z f_x(x) f_y(z - x) dx \quad (24)$$

64. Equations 12 and 17 can now be substituted into Equation 24 to achieve a combined PDF

$$p\sigma'_c(z) = \int_0^z p\sigma'_s(x) p\sigma'_p(z - x) dx \quad (25)$$

The resulting output from the convolution integral is a combined stress PDF for static and pulsating stress responses. The convolution is performed numerically in CAUDAID and the resulting combined PDF is then numerically integrated to get a combined exceedance probability function (CEPF). This CEPF is used to determine a design stress given the design probability of exceedance.

Design probability of exceedance

65. Choosing the design stress from the CEPF requires selection of a design probability of exceedance, which is based on the structure's design life and the number of armor units allowed to break in any given time period. Markle and Davidson (1983) state that a dolos armor layer will continue to remain stable provided dolos breakage does not exceed a uniform 15 percent in the top layer, 15 percent in the bottom layer, and 7.5 percent in both layers or clusters of 5 individual units. One could infer, then, that the design probability of exceedance E for a dolos armor layer must be significantly less than 15 percent for an armor layer. In Appendix A, for Crescent City, the design stress for the 42-ton dolosse is calculated from the CEPF using a probability of exceedance of 2 percent.

Fatigue

66. A thorough review of general fatigue concepts should be done prior to estimation of a fatigue coefficient. General fatigue theory is contained

in ASTM C39-83b (ACI Committee 215R-74 (1981)). Fatigue in concrete dolosse has been investigated by Tait and Mills (1980) and Burcharth (1984). Howell et al. (1992) summarize and compare the results of Burcharth and Tait and Mills. Tait and Mills' results include pulsating fatigue S-N (stress versus number of cycles to failure) curves, while Burcharth's results compare impact fatigue with Tait and Mills' results. Because impact stresses are not included in this design methodology, only the pulsating results of Tait and Mills are used.

67. From the above comparison of fatigue pulsating S-N curves, based on the research by Tait and Mills and Burcharth, a fatigue strength reduction coefficient can be developed for pulsating loads as

$$k_F = -0.067 \log_{10} N + 1 \quad (26)$$

where N is the number of design storm pulsating cycles occurring within the design life. The value of N can be determined for a given coastal region from knowledge of the characteristics of local storms.

Dolos material properties

68. The preliminary design critical strength in the dolos will be the product of the concrete tensile strength f' , and the fatigue reduction factor, k_F . The design tensile strength is highly variable, depending on concrete quality. To prevent corrosion of the concrete through chemical reaction with seawater and reinforcing steel, the concrete must be dense and watertight. Mixing and curing procedures as well as water-cement ratios, aggregate quality, and admixture types and amounts are therefore extremely important. Procedures for selection of concrete materials are given in EM 1110-2-2000 (US Army Corps of Engineers).

69. Tensile strength tests consist of indirect measurements including flexure tests of beams, splitting tests of small cylinders, and direct measurements including pulling tests of cylinders and rectangular blocks. Tensile strength tests, in general, achieve widely varying results depending on the particular concrete mix, the care taken in making the sample, and the testing procedure used. Also, it is generally accepted that direct tensile test results are not as reliable as indirect tests because of the difficulty in gripping the sample. Finally, tensile strengths based on tests of ideal specimens may not be representative of the actual tensile strength because of the highly complex stress state within the slender CAUs. The actual strength

in slender CAUs is generally less than the strength determined from these ideal tests.

70. Kendall and Melby (1990) give a modulus of rupture or pure bending tensile strength of $f'_r = 984$ psi for the Crescent City dolosse. The splitting tensile strength can be estimated as $f'_t = 0.73 f'_r = 718$ psi. This value can be thought of as a conservative design strength for the Crescent City case.

71. High-strength concrete is generally with reference to the compressive strength, which might be on the order of 10,000 psi. Because CAUs are generally unreinforced, the CAU designer is interested in the tensile strength. While the American Concrete Institute gives the design relationship for the modulus of rupture of normal weight concrete as $f'_r = 7.5\sqrt{f'_c}$ (ACI-9.5.2.3), where f'_c is the compressive strength in psi, this relationship is not necessarily conservative for high-strength concrete. Saucier (1984) has shown that the ratio between tensile and compressive strengths for high-strength concrete can be maintained. With the use of quality materials, low water-cement ratios, high-range water-reducing admixtures, and very fine silicon-dioxide powder, or silica fume, compressive strengths as high as 15,000 psi with corresponding moduli of rupture as high as 1,200 psi can be achieved with little loss in workability. Therefore, high-strength concrete may be a viable alternative for some designs.

72. High-unit-weight concrete may be a design alternative but very little research has been done in this area. High-unit-weight aggregate could be added to the concrete to achieve more hydraulically stable armor units. From the Hudson equation it can be seen that the armor unit stable weight is inversely proportional to the density cubed. Increasing the concrete density is therefore highly advantageous. As an example, for the Crescent City dolosse, increasing the unit weight from 150 pcf to 160 pcf provides a 23-percent decrease in the dolos design volume. The design stress decreases by 4 percent for this 6.7-percent increase in unit weight.

73. The effect of temperature differentials in curing concrete dolosse was investigated by Norman and Alexander (1985). Their conclusion was that, for Crescent City dolosse of waist ratio 0.32, there is little effect on strains from construction-related temperature differentials within the dolosse. For higher waist ratio dolosse, this topic may require further study.

Factor of safety

74. The design stress from the joint EPF can be compared to the fatigue-reduced strength as follows:

$$\sigma'_c \gamma C \leq k_F f'_t \quad (27)$$

or

$$FS = \frac{k_F f'_t}{\sigma'_c \gamma C} \quad (28)$$

75. If the stress exceeds or is near the strength, the factor of safety will be near to or less than 1 and the designer will iterate back through the preliminary design phase. For greater factors of safety, selection or rejection of the design may hinge on economics. The conclusion of the preliminary design phase could include a comprehensive economic analysis, which may lead to more iteration to determine the optimum dolos.

Reinforcement

76. If the internal stresses are too high within an unreinforced dolos, the designer may elect to incorporate some sort of structural reinforcement. Several types of reinforcement that have been investigated for dolosse include fiber, rebar, and post-tension tendons. Fiber reinforcement can add significantly to the strength but it can also be of negligible value. Fibers were used in the Crescent City dolosse and the Humboldt, California dolosse. There is no evidence that these dolosse have performed better or worse than similar unreinforced units.

77. The primary disadvantage of fiber reinforcement is that the fibers are distributed uniformly across the section and throughout the dolos. Because steel reinforcement of any kind is relatively expensive, in conventional concrete design, steel reinforcement is generally placed at locations of highest stress. Fibers are therefore not a very efficient use of reinforcing steel. But, depending on the dolos boundary condition, position, and orientation, the maximum stress can occur at a number of locations in the dolos, with the location of highest tensile stress being random. But because flexural shear stresses are, in general, small the maximum stresses will occur close to the outer fibers of the cross section. Therefore, having fibers throughout the dolos may still be an inefficient use of reinforcement. But fibers tend to be less expensive than the other forms of reinforcing. A list

of publications concerning the use of fiber reinforcement is given in Howell et al. (1992).

78. Conventional rebar reinforcement has been used in dolosse and adds significantly to the strength of the units. The advantage of rebar is that it significantly increases the tensile strength of the cross section. The main disadvantages of conventional steel reinforcement are:

- a. Steel must be put in equal amounts throughout the dolos cross section because of the random location of the maximum stress.
- b. Because the loads are unknown, the amount of steel must be overestimated.
- c. In order for the steel to be effective, the unit must crack, thereby allowing corrosive seawater to come in contact with the steel.

For these reasons, the cost of conventional reinforcing can be prohibitively high.

79. Pre-stressing or post-tensioning steel tendons within the dolosse has been shown to be effective at increasing the cross-section strength (McDougal, Melby, and Tedesco 1987), but the logistics of economically tensioning the tendons have not been investigated.

80. Because this design procedure does not quantify the loads on a dolos, specification of conventional reinforcement is not part of these design methods. The design methodology does lend itself nicely to strength enhancement methods, though. The strength enhancements that can be implemented include high-strength concrete, fiber reinforcing, and prestressing or post-tensioning. These enhancements can be implemented during the final design process if the design stress is too high. Follow-on reports that are currently in preparation will investigate strength enhancement alternatives and compare the competing alternatives on a cost basis (Melby and Turk 1992).

Intermediate Dolos Design

81. The intermediate design phase, illustrated in Figure 9, will consist of simultaneously measuring the dolos structural response and hydrodynamic stability in physical model studies, where necessary. The designer must determine if the costs involved with measuring the dolos structural

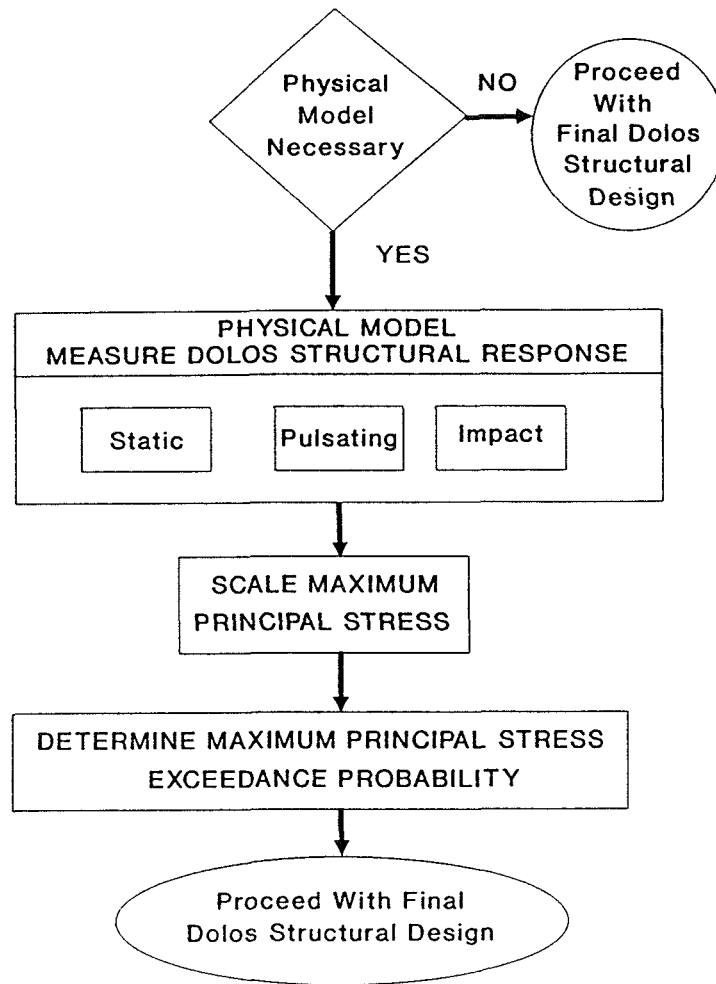


Figure 9. Dolos intermediate structural design

response in the physical model justify the benefits. If a moderately sophisticated hydrodynamic stability physical model study is done and if the appropriate dolos structural instrumentation for the model-sized units is available, measuring structural response in the physical model adds little to the hydraulic testing costs. As parametric data become incorporated into the design procedure, the need for structural measurements in the physical model should decrease.

82. Because most of the above CAU design methods involve costly or unverified techniques, the instrumentation of small-scale model armor units is becoming an increasingly viable option, particularly with advances in small-scale instrumentation technology (Markle 1990a). Use of the load cell

structural instrumentation reduces the scaling requirements to a manageable level. The only material properties that must be modeled for measurement of static and wave-induced responses using this technique are density and surface friction. The gross structural response in the form of moments is read directly from the calibrated load cell. The Crescent City dolos design procedure therefore includes measurement of dolos static and pulsating structural response in the physical model using the load cell instrumentation.

83. Scaling of the hydrodynamic response of armor units where inertial and gravity forces predominate generally follows the Froude law (Hudson 1958). Wave forces on armor units include buoyancy, drag, inertia, and kinetic or wave-slamming components (Melby 1987). For waves that approach and exceed their limiting steepness, the kinetic or wave slamming and inertial forces on armor units in the splash zone begin to be dominant (McDougal, Melby, and Tedesco 1987). Froude similitude will, in general, be conservative in these conditions. Froude scaling for structural response in these conditions will also, in general, be conservative.

84. In the small-scale physical model, load cell technology will be utilized to measure structural response to static, pulsating, and impact loads. Use of the load cell is described in Markle (1990b) and Howell, Rhee, and Rosati (1990). Burcharth and Howell (1988) describe some general stress measurement and analysis techniques. Measuring and analyzing the static response can be done using the methods outlined in Melby, Rosson, and Tedesco (1990). Static, pulsating, and impact responses can all be measured simultaneously and extracted from each time series using the following techniques. The individual response EPFs can be combined to form a joint EPF in the final design phase.

85. The method currently used to extract the static, pulsating, and impact stresses from a single stress record is reasonably simple. The static stresses can be obtained as the mean of each detrended time series, provided the response is fairly symmetric about this mean value.

86. The impact response can be observed as spikes in the time series and can be removed using a spike removal technique. Note that a very high sampling rate is required to obtain the entire impact response. Also, the model dolos impact response will be distorted due to the inclusion of structural instrumentation and incorrect scaling of material elasticity. Care must be taken in interpreting the model impact results. A scaling factor that

would take these structural distortions into account is currently being investigated. The reader should also note that the impact response will be correlated with the hydrodynamic stability. Therefore, the impact response will be a function of the same variables as is the hydraulic stability. These variables include wave direction, wave length, wave shape, structure slope, spectral width, etc. What is left after detrending, demeaning, and despiking the time series is the pulsating response.

87. Many tests are required in order to determine a statistically representative sample of the maximum stresses in the armor layer. The number of these tests can be reduced by utilizing results of recent parametric studies. The maximum static stresses will be in the underlayer. To test for static stress, several instrumented dolosse can be placed on a small ramp at the prototype slope and density, along with many noninstrumented dolosse. The static response can then be measured for both the nested and unnested conditions. The nested configuration can be achieved by shaking the ramp. Scaling factors for wedging loads, size, and material density can be applied to these data to determine the maximum static stress distribution.

88. Recent studies indicate that the pulsating stresses are maximum above and near the still-water level. Pulsating and impact structural measurements can therefore be limited to two to three dolosse placed at and near the still-water level. Also, for pulsating and impact responses, no additional wave conditions beyond those used to test hydrodynamic stability need be run. The individual nondimensional design EPFs for the static, pulsating, and impact responses will be generated from the model data in this intermediate design phase. Techniques for fitting the best distribution to the data are described in Burcharth (1985) and include choosing a distribution, comparing plotting rules, noting variations and uncertainties, and quantifying distribution errors.

89. Proper attention to scaling is required in order for the results of the small-scale structural measurements to be meaningful. Scott, Turcke, and Baird (1990) and more recently, Anglin et al. (1990) have reported the results of a large series of parametric physical model tests using small-scale model dolosse. The results show static stresses, when scaled to the prototype level, far below those measured in the Crescent City prototype dolosse. This difference may be attributed to the improper scaling of static wedging loads in the small-scale units. Melby, Rosson, and Tedesco (1990) compared Crescent

City prototype dolos static response with FEM models using geometrically identical boundary conditions. The FEM stresses, which were due only to self-weight loads, were 10 to 20 percent of the prototype stresses, indicating that the bulk of the prototype static stress is due to the wedging loads. The wedging loads are a function of the dolos weight, dolos slenderness or waist ratio, unit-to-unit friction, and several other secondary variables. Scaling the unit surface friction correctly is therefore critical, but difficult, because it increases with time due to nesting and progressive exposure of aggregate at the spalled contact surfaces. Because the unit-to-unit friction is difficult to model in the small-scale units and little is known about the long-term changes of the surface friction coefficient, current design guidance must rely on prototype level static measurements.

Final Dolos Design

90. In the final design phase, illustrated in Figure 10, the individual EPFs from the physical model study will be combined into a single design EPF using the methods outlined in Part II. The maximum likely stress

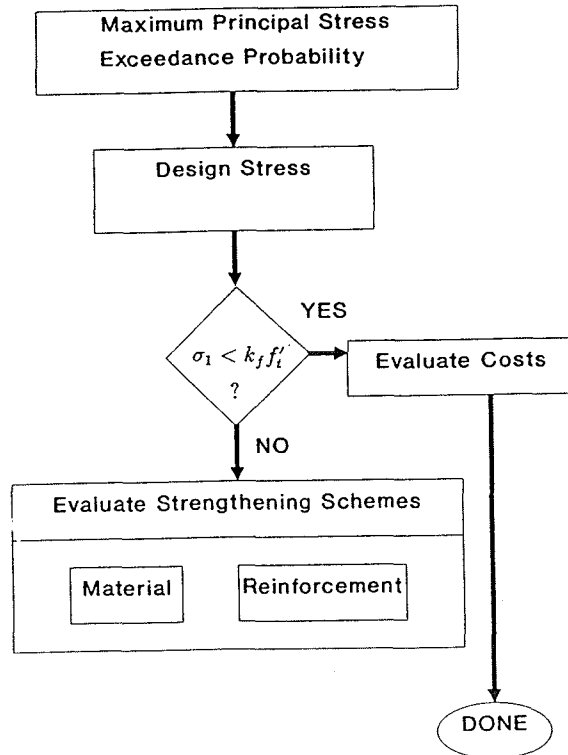


Figure 10. Dolos final design.

can then be determined from this design distribution and compared to the fatigue-reduced strength using Equation 28. If the stress exceeds the strength, the designer must implement some strengthening scheme. Two possible strengthening schemes include higher strength concrete and reinforcement. Possible reinforcement schemes include fiber, steel rebar, and posttensioning, as discussed earlier. Conventional structural design techniques can be used to determine the effect and the relative benefits of these strengthening schemes. The final step in the dolos structural design process could be another economic analysis.

PART III: APPLICATION OF THE DESIGN METHODOLOGY

General Design Diagrams

91. Although the design methods outlined herein have been packaged in a user-friendly PC computer program, it is useful to preplot some of the results in design diagrams. In this section the figures were generated using the program CAUDAID, which solves the nondimensional Equations 12 and 17 using statistics given in Table 4. In all of the calculations a waist ratio of 0.32 and two armor layers were used. A structure slope of 1:2 was used for the stability calculations.

92. Figure 11 shows stress versus dolos weight for various Hudson equation stability coefficients. These curves were generated by computing stable wave heights for various dolos weights. The design stresses corresponding to these waves and weights were then computed by combining the associated static and pulsating stress EPFs. Thus, the curves represent both structurally and hydrodynamically stable dolosse.

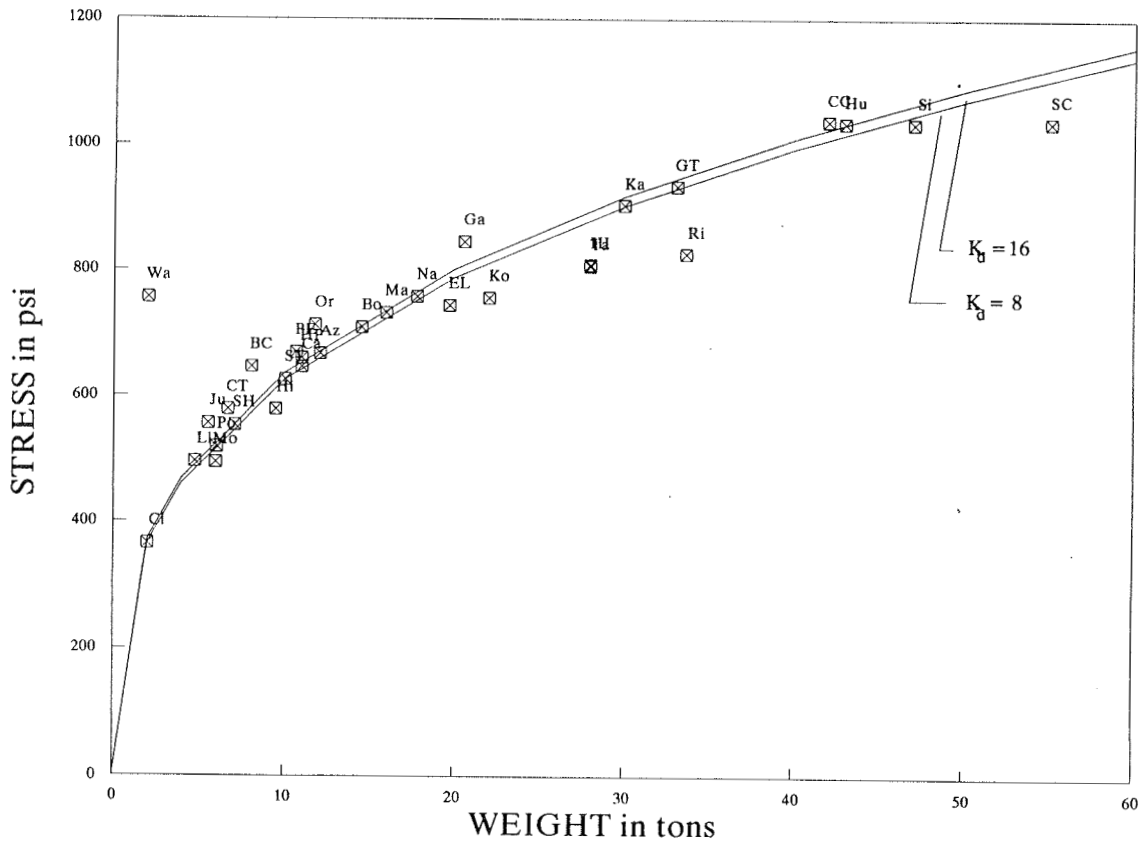


Figure 11. Dolos stress versus weight

93. It can be seen from this figure that the stress increase with weight for small dolosse is dramatic but that the increase becomes almost linear above about 15 tons. For normal strength concrete having a tensile rupture strength of approximately 600 psi, stable dolosse below 10 tons are not at risk structurally, while those above 20 tons require strengthening. The various points plotted on this figure are prototype cases and they will be discussed in the following section.

94. Figure 12 shows a typical dolos design diagram where the hydrodynamically stable dolos weight and the structurally stable dolos weight are plotted as two separate curves versus wave height.

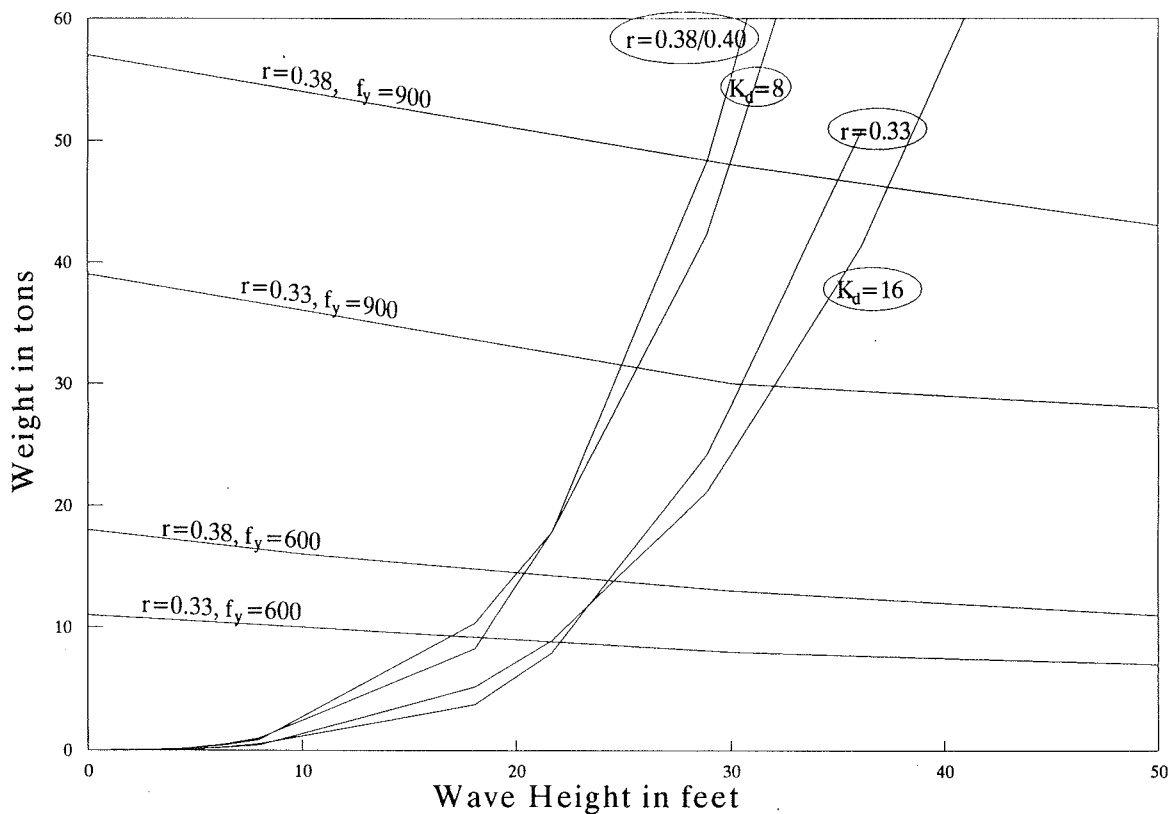


Figure 12. Dolos design diagram

95. The strength curves are nearly horizontal, angling slightly down to the right. The hydrodynamic stability curves begin at the origin and increase at an exponential rate to the right. The design envelope would be below the appropriate strength curve and to the left of the appropriate hydrodynamic stability curve. This plot gives the stability for three waist ratios using the results of Zwamborn, Scholtz, and Claasens (1988) as well as

that given by the Hudson equation for two different stability coefficients. The strength portion of the design envelope is plotted for two different concrete tensile rupture strengths, $f'_y = 600$ psi and $f'_y = 900$ psi . It can be seen that the increase in waist ratio from 0.33 to 0.38 has only a minor effect on the stability but increases the acceptable weight by 63 percent for 600-psi concrete and 46 percent for 900-psi concrete. It is also evident from Figure 12 that stress changes more rapidly with weight for lighter dolosse than for heavier dolosse and that wave height has only a minor effect on the combined static and pulsating design stress.

Application of Design Methods to Existing Dolos Structures

96. Table 5 shows design data for dolos structures throughout the world as given in Zwamborn, Bosman, and Moes (1980), and Markle and Davidson (1983). In these tables ABR is the location abbreviation used in the following figures, H is the design wave height, T the design wave period, d the toe water depth, $\cot(\alpha)$ the structure slope, and PLACE is the placement as follows:

MBT, MBH, MBHT - Main breakwater trunk, head, and head and trunk, respectively

SBT, SBH - Secondary breakwater trunk and head, respectively

In Table 5, r is the waist ratio, phi is the placement density, S is the specific gravity, STRN is the concrete compressive strength, num is the number placed, and reinf is the structural reinforcement used.

97. Table 6 shows the results of applying the dolos structural design procedure to these structures. The stresses shown are combined static and pulsating design tensile stress levels for a probability of exceedance of 2 percent. In Table 6, W is the dolos weight and $STRN = f'_y$ is the rupture tensile strength computed using the compressive strength, f'_c , in the formula

$$f'_y = 200 + 0.09 f'_c \quad (29)$$

98. Figure 11, showing stress versus dolos weight for various Hudson equation stability coefficients, also plots most of the structures listed in Table 6. It can be seen from this figure that most of the structures throughout the world have design stress levels between 400 and 1,000 psi without impacts.

Table 5

Dolos Structures Throughout the World

LOCATION	COUNTRY	ABR	H ft	T	d ft	COT a	PLACE	r	phi	WEIGHT ton	S	STRN psi	NUM	REINF	% BROKE			DATE PLACED
															cast	place	service	
Azzawiya	Libya		19.7		16.4		1.5 MBT			6.06								1977
Azzawiya	Libya	Az	23.0		19.7		2 MBH			12.13								1977
Baie Comeau Quebec	Canada		32.8		32.8		1.5 MBT	0.3	1.14	4.96	2.4	7830	3000					1976
Baie Comeau Quebec	Canada	BC	32.8		32.8		2 MBH	0.3	1.15	8.05	2.4	7830	200					1976
Botany Bay	Australia	Bo	25.6		37.1		MBT	0.32		14.55								
Cap Aux Meules	Canada				18.0		1.5 MBT			3.97			7600		1.00	1.00	0.00	1970
Cap Aux Meules	Canada				20.0		1.5 MBH			6.06			4600					1970
Cape Town	SA		6.6	12	19.7		1.5 MBT	0.32	1.13	3.31	2.4	4350	8631		0.80	0.10	0.00	1972
Cape Town	SA	CT	14.8	12	28.9		1.5 MBH	0.31	1.47	6.62	2.4	4350	27270		0.30	0.10	0.00	1972
Cape Town	SA		8.2	12	2.6		1.5 SP	0.32	1.13	3.31	2.4	4350	9366					1972
Carboneras	Spain	Ca	23.0		54.1		1.3 MBT			11.03								
Crescent City CA	US		35.0	18	30.0		2 MBT	0.32		40.00		6250	246	none	2.00	9.00	most	1974
Crescent City CA	US	CC	35.0	18	30.0		5 MBT	0.32		42.00	2.4	6250	500	fiber	0.00	0.00	1.00	1985
Cleveland Harbor OH	US	CI	13.4	8.8	30.0		2 MBHT	0.32		2.00			29500	none	0.00	0.00	1.69	1980
East London	SA		27.9	12	23.0		1.25 MBT	0.34		19.73	2.36	4350	2000	rails(few)	0.20	0.50	0.30	1964
East London	SA	EL	27.9	12	23.0		1.25 MBH	0.34		19.73	2.36	4350	0	rails(few)	0.20	0.50	0.30	1964
Gans Bay	SA		19.7	12	31.8		1.5 MBT	0.3	1.16	18.85	2.4	4596.5	1651			4.00	0.50	1970
Gans Bay	SA	Ga	19.7	12	38.4		1.5 MBH	0.3	1.09	20.61	2.4	4596.5	1500					1970
Gans Bay	SA				28.5		1.25 MBIS	0.33	1.13	4.96	2.4	4596.5	1000					1970
Giola Tauro	Italy		26.2	11.5	49.2		1.7 MBT	0.32		16.54								1978
Giola Tauro	Italy	GT	29.5	11.5	65.6		2 MBH	0.32		33.08								1978
Giola Tauro	Italy		26.2	11.5	49.2		1.7 SBT	0.32		16.54								1978
Giola Tauro	Italy		29.5	11.5	65.6		2 SBH	0.32		33.08								1978
Hay Point	Australia		20.0	10	33.1		1.5 MBT	0.32	0.74	8.82	2.35	5075						1978
Hay Point	Australia	HP	26.6	10	33.1		2 MBH	0.32	0.73	11.03	2.35	5075						1978
High Island	Hong Kong	HI	35.1	15	47.9		2 MBT	0.35	1.16	28.01			6619			0.80		1973
Hirtshals	Denmark	Hi		8	31.2		1.5 MBT	0.33	1.02	9.48	2.35	4973.5	1000		0.30	0.30	0.04	1972
Hirtshals	Denmark	Hi	12.8	8	31.2		2 MBH	0.33	1.02	9.48	2.35	4973.5	1600		0.40	1.40	0.20	1972
Humboldt Bay CA S	US		40.0	16			5 MBHT	0.32	11/1000	42.00			22	none			40.00	1972
Humboldt Bay CA S	US		40.0	16			5 MBHT	0.32	11/1000	42.00			1423	Conv			0.91	1972
Humboldt Bay CA S	US		40.0	16			5 MBHT	0.32	11/1000	43.00			1090	Conv				1972
Humboldt Bay CA N	US		40.0	16			5 MBHT	0.32	11/1000	42.00			4	none			0.90	1972
Humboldt Bay CA N	US		40.0	16			5 MBHT	0.32	11/1000	42.00			1271	Conv			0.94	1972
Humboldt Bay CA N	US		40.0	16			5 MBHT	0.32	11/1000	42.00			17	fiber			0.00	1972
Humboldt Bay CA N	US	Hu	40.0	16			5 MBHT	0.32	11/1000	43.00			967	Conv			0.00	1972
Jubail	Jubail	Ju	16.4		29.5		2 MBH			5.51							0.00	1976

(Continued)

Table 5 (Concluded)

LOCATION	COUNTRY	ABR	H ft	T	d ft	COT a	PLACE	r	phi	WEIGHT ton	S	STRN psi	NUM	REINF	% BROKE			DATE PLACED
															cast	place	service	
Kahului Harbor HI W	US	Ka	34.0	18		2.3 MBH	0.32			30.00			257	Conv			2.55	1977
Kahului Harbor HI W	US		34.0	18		2.3 MBT	0.32			20.00			291	Conv				1977
Kahului Harbor HI E	US		34.0	18		2.3 MBH	0.32			30.00			610	Conv			0.00	1977
Kahului Harbor HI E	US		34.0	18		2.3 MBT	0.32			20.00			164	Conv			0.32	1977
Kahului Harbor HI E	US		34.0	18		2.3 MBT	0.32			6.00			455	none			0.44	1977
Koeberg Nuclear Power Sta	SA			16		1.5 MBT	0.34	1.19		16.54	2.4	7250	2580		1.00	2.00	5.00	1980
Koeberg Nuclear Power Sta	SA	Ko	23.0	16		1.5 MBH	0.34	1.15		22.05	2.4	7250	1609		1.00	2.00	5.00	1980
Koeberg Nuclear Power Sta	SA			16		1.5 SBT	0.34	1.16		6.62	2.4	7250	1248		1.00	2.00	5.00	1980
Koeberg Nuclear Power Sta	SA			16		1.5 SBH	0.34	1.19		16.54	2.4	7250	2007		1.00	2.00	5.00	1980
Kuwait	Kuwait					1.5 MBT	0.36			1.54								1974
Llanddulas	UK	LI	19.7			2 SP	0.32			4.74								
Mackay	Australia					1.5 MB				8.82								
Manasquan NJ	US	Ma	25.0	13		2 MBHT	0.32	23/1000		16.00			1326	Conv			0.40	1980
Mossel Bay	SA		9.8			1.5 MBT	0.33			2.98			3420					1969
Mossel Bay	SA	Mo	9.8			1.5 MBH	0.33			5.95			2630					1969
Nawiliwili Harbor Kauai HI	US	Na	24.0	15		2 MBHT	0.32			17.80			934	None				1977
Oranjemund	SW Africa	Or	25.3	11.5	18.0	1.5 MBH	0.31	1		11.80	2.55	5800	3267			5.00		1977
Port Elizabeth Coast	SA					1.5 SP	0.3	1.1		3.20	2.39	4495	13343		2.25			1968
Port Elizabeth Harbor	SA	PE	21.0	12	50.2	1.7 MBH	0.31	1.02		10.69	2.38	5365	8500		0.45			1968
Pohoiki Bay Hawaii HI	US	Po	12.0	20		2				6.00			210	none		0.02		1979
Richards Bay	SA		23.6	11.5	53.5	1.5 MBT	0.33	1.04		22.41	2.4	5510	13397		0.38	0.96	0.01	1976
Richards Bay	SA	Ri	29.5	11.5	58.7	2 MBH	0.37	1.04		33.62	2.4	5510	2194			0.30	0.01	1976
Richards Bay	SA		23.0	11.5	16.7	1.5 SBT	0.33	1.04		5.60	2.4	5510	8832		0.14	0.67	0.01	1976
Richards Bay	SA		23.0	11.5	26.9	2 SBH	0.33	1.04		16.81	2.4	5510	942		0.21	1.36	0.01	1976
Saline di Montebello	Italy				32.8	MBT,H	0.32			16.54								
San Ciprian	Spain		42.7	15.5	68.9	2 MBT	0.35	0.98		55.13	2.41	4930	17351		0.70	1.00	5.00	1979
San Ciprian	Spain	SC	42.7	15.5	72.2	2 MBH	0.35	0.98		55.13	2.41	4930			0.70	1.00	5.00	1979
San Ciprian	Spain		42.7	15.5	76.4	2 SB	0.35	0.98		55.13	2.41	4930			0.70	1.00	5.00	1979
Sines Portugal	PORT		45.8	13.5	90.0	1.5 MBT	0.35	1.18		47.06	2.55	7105	15000	None	0.50	1.50	5.00	1979
Sines Portugal	PORT	Si	45.8	13.5	90.0	2 MBH	0.35	1.18		47.06	2.55	7105	4000	None	0.50	1.50	5.00	1979
St Helena Bay Cape Province	SA	SH	20.0		31.8	1.75 MBT	0.33	1.02		7.06	2.43	5002.5						1968
St Thomas	Virgin Islands		23.0		88.6	1.5 MBT				6.06								1979
St Thomas	Virgin Islands	ST	23.0		88.6	1.5 MBH				10.03								1979
Table Bay	SA	Ta	31.3	16	16.0	1.5 MBT	0.36	19/1076		28.00	2.45	7000		toe,rail			2.00	1988
Tristan de Cunha	South Atlantic					MBT				2.21								
Turton Bay	SA					SP				3.31								1973
Waianai Harbor Oahu HI	US	Wa	11.8	16		2 MBHT	0.32			2.00			6630	None	0.00	0.71	1.85	1979

Table 6

Design Stresses for Various Dolos Applications

LOCATION	ABR	H ft	r	W ton	S	STRS psi	STRN psi
Azzawiya	Az	23.0		12.13	2.4	668	
Baie Comeau Quebec	BC	32.8	0.3	8.05	2.4	647	904.7
Botany Bay	Bo	32.8	0.32	14.55	2.4	710	
Cape Town	CT	25.6	0.31	6.62	2.4	579	591.5
Carboneras	Ca	23.0		11.03	2.4	647	
Crescent City CA	CC	35.0	0.32	42.00	2.45	1038	930
Cleveland Harbor OH	CI	13.4	0.32	2.00	2.4	366	
East London	EL	27.9	0.34	19.73	2.36	745	591.5
Gans Bay	Ga	19.7	0.3	20.61	2.4	846	613.69
Gioia Tauro	GT	29.5	0.32	33.08	2.4	934	
Hay Point	HP	26.6	0.32	11.03	2.35	661	656.75
High Island	HI	35.1	0.35	28.01	2.4	810	
Hirtshals	Hi	12.8	0.33	9.48	2.35	579	647.62
Humboldt Bay CA N	Hu	40.0	0.32	43.00	2.4	1035	
Jubail	Ju	16.4		5.51	2.4	557	
Kahului Harbor HI W	Ka	34.0	0.32	30.00	2.4	904	
Koeberg Nuclear Power Sta	Ko	23.0	0.34	22.05	2.4	757	852.5
Llandulas	LI	19.7	0.32	4.74	2.4	496	
Manasquan NJ	Ma	25.0	0.32	16.00	2.4	733	
Mossel Bay	Mo	9.8	0.33	5.95	2.4	495	
Nawiliwili Harbor Kauai HI	Na	24.0	0.32	17.80	2.4	759	
Oranjemund	Or	25.3	0.31	11.80	2.55	714	722
Port Elizebeth Harbor	PE	21.0	0.31	10.69	2.38	670	682.85
Pohoiki Bay Hawaii HI	Po	12.0		6.00	2.4	520	
Richards Bay	Ri	29.5	0.37	33.62	2.4	827	695.9
San Ciprian	SC	42.7	0.35	55.13	2.41	1037	643.7
Sines Portugal	Si	45.8	0.35	47.06	2.55	1034	839.45
St Helena Bay Cape Province	SH	20.0	0.33	7.06	2.43	554	650.23
St Thomas	ST	23.0		10.03	2.4	627	
Table Bay	Ta	31.3	0.36	28.00	2.45	807	830
Waianai Harbor Oahu HI	Wa	11.8	0.32	2.00	2.4	756	

99. Figure 13 shows most of the structures listed in Table 6 on a design diagram. The hydrodynamic stability line is based on the Hudson equation for a stability coefficient of $K_d = 16$ simply to give some idea of the relative stability of the different applications. Strength lines are plotted for a waist ratio of $r = 0.33$ and strengths of $f'_t = 600$ and 900 psi. Note that the larger dolosse with weights above 30 tons generally fall outside of both the strength and stability lines, medium-sized dolosse are at the corner of the design envelope, and small dolosse with weights below 10 tons fall within both the strength and stability curves. It is likely that

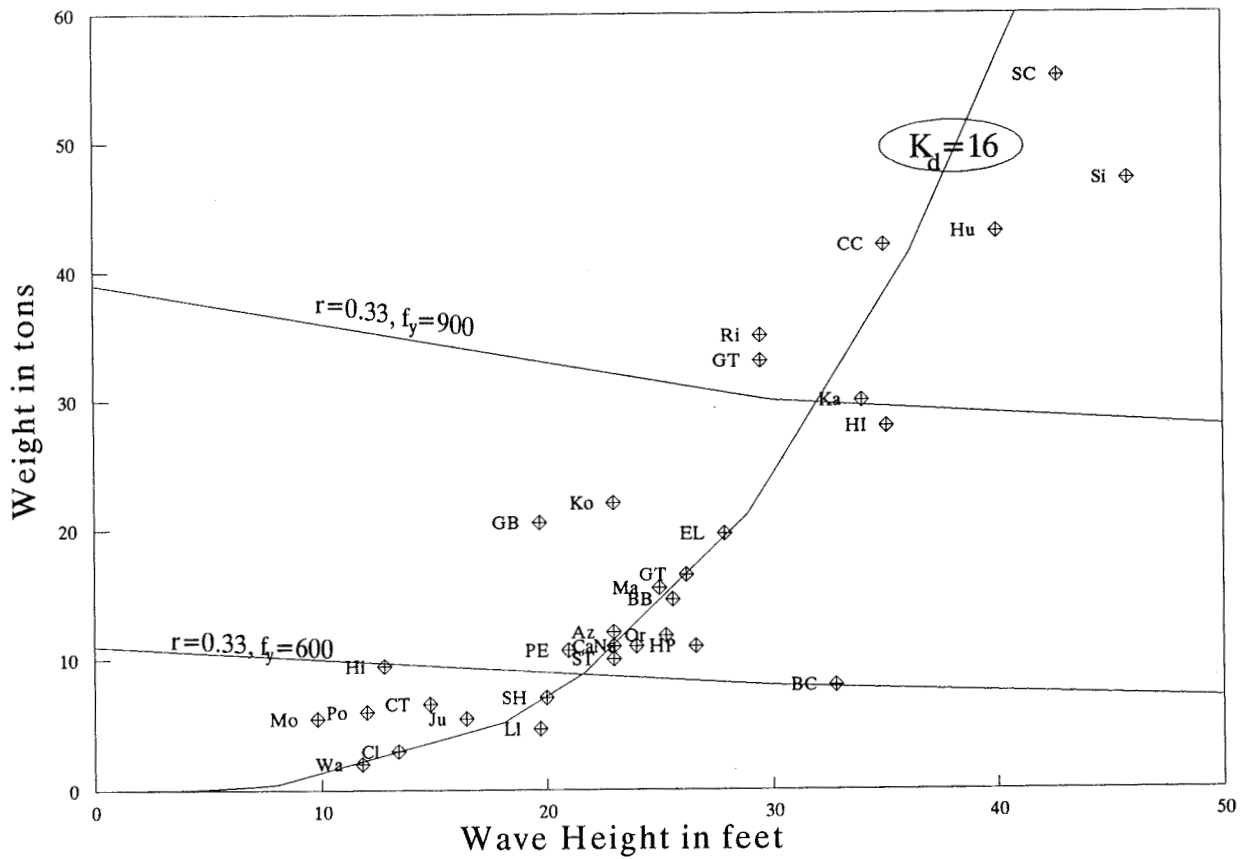


Figure 13. Dolos design diagram with worldwide dolos applications

inclusion of impact response would alter this plot significantly but that dolosse above 20 tons simply could not tolerate any impacts. Also, reinforcing and strength enhancements would improve all the prototype applications on this figure.

PART IV: SUMMARY AND CONCLUSIONS

100. This design procedure includes statistical methods for determining a design stress in a dolos armor layer. The methods characterize the structural response as a single parameter: the maximum principal tensile stress in each dolos. Using this approach, the dolos shape can be optimized for structural integrity and hydrodynamic stability, and the design can be verified in the physical model. Also, the structural response to the most significant loading mechanisms can be computed separately and the individual statistical distributions combined to yield a design stress distribution. The design stress is computed using this design stress distribution and then compared to a fatigue-reduced strength. The iterative optimizing design process can be accomplished using a user-friendly PC-based computer program.

101. It is shown that unreinforced normal-strength dolosse above 20 tons are often underdesigned with respect to strength and can tolerate only slight movement and the associated impacts. It is also shown that increasing the dolos waist ratio can add significantly to the unit's strength, while sacrificing little hydrodynamic stability, and that large dolosse over 30 tons require some strengthening scheme. The methods discussed in this paper provide a complete procedure for determining a design stress within a hydrodynamically stable dolos and can be used as an outline in the design of other slender armor unit shapes.

REFERENCES

- ACI Committee 215R-74. 1984 (revised 1981). "Considerations for Design of Concrete Structures Subjected to Fatigue Loading," American Concrete Institute Manual of Concrete Practice.
- Anglin, C. D., Scott, R. D., Turcke, D. J., and Turcke, M. A. 1990. "The Development of Structural Design Criteria for Breakwater Armour Units," American Society of Civil Engineers/WPCO Seminar on Stresses in Concrete Armor Units, New York.
- Baird W. F., Caldwell, J. M., Edge, B. L., Magoon, O. T., and Treadwell, D. D. 1980. "Report on the Damages to the Sines Breakwater, Portugal," Proceedings, 17th Coastal Engineering Conference, American Society of Civil Engineers, No. 3, March.
- Burcharth, H. F. 1981. "A Design Method for Impact Loaded Slender Armour Units," Bulletin No. 18, Laboratoriet for Hydraulik og Havenebygning, University of Aalborg, Denmark.
- _____. 1983. "Material, Structural Design of Armour Units," Laboratoriet for Hydraulik og Havenebygning, University of Aalborg, Denmark.
- _____. 1984. "Fatigue in Concrete Armour Units," Laboratoriet for Hydraulik og Havenebygning, University of Aalborg, Denmark.
- _____. 1985. "On the Reliability of Rubble Mound Breakwater Design Parameters," Laboratoriet for Hydraulik og Havenebygning, University of Aalborg, Denmark.
- Burcharth, H. F., and Howell, G. L. 1987 and 1988. "On Methods of Establishing Design Diagrams for Structural Integrity of Slender Complex Types of Breakwater Armour Units," Proceedings, Workshop on Measurement and Analysis of Structural Response in Concrete Armor Units, US Army Engineer Waterways Experiment Station, Coastal Engineering Research Center, Vicksburg, MS, Seminaire International Entretien des Infrastructure Maritimes, Casablanca, Morocco.
- Burcharth, H. F., and Liu, Z. 1990. "A General Discussion of Problems Related to the Determination of Concrete Armour Unit Stresses Including Specific Results Related to Static and Dynamic Stresses in Dolosse," American Society of Civil Engineers/WPCO Seminar on Stresses in Concrete Armor Units, New York.
- Coastal Engineering Research Center. 1992. "Movement and Static Stresses in Dolosse," Coastal Engineering Technical Note III-42, US Army Engineer Waterways Experiment Station, Coastal Engineering Research Center, Vicksburg, MS.
- Holzhausen, A. H., and Zwamborn, J. A. 1991. "Stability of Accropode and Comparison with Dolosse," Coastal Engineering Journal, Vol 15, pp 59-86.

Howell, G. L. 1985. Proceedings, Workshop on Measurement and Analysis of Structural Response in Concrete Armor Units, US Army Engineer Waterways Experiment Station, Vicksburg, MS.

_____. 1986. "A System for the Measurement of the Structural Response of Dolos Armour Units in the Prototype," The Dock and Harbor Auth., Vol 67, No. 779, pp 6-11.

_____. 1988. "Measurements of Forces on Dolos Armor Units at Prototype Scale", Proceedings, 21st International Conference on Coastal Engineering, American Society of Civil Engineers, New York.

Howell, G.L., Melby, J.A., Rosati, J., Markle, D., Rhee, J., Kendall, T., Bevins, T., Johnson, W., and Norman, C. "Crescent City Prototype Dolos Study: Final Report," in preparation, US Army Engineer Waterways Experiment Station, Vicksburg, MS.

Howell, G.L., Rhee, J.P., and Rosati, J. 1990. "Stresses in Dolos Armor Units," American Society of Civil Engineers/WPCO Seminar on Stresses in Concrete Armor Units, New York.

Hudson, R.Y. 1958. "Design of Quarry Stone Cover Layers for Rubble-Mound Breakwaters," Research Report No. 2-2, Jul 58, US Army Engineer Waterways Experiment Station, Vicksburg, MS.

Johnson, W.G., and Bevins, T.L. 1990. "Stacking Analysis for Dolosse," American Society of Civil Engineers/WPCO Seminar on Stresses in Concrete Armor Units, New York.

Kendall, T.R., and Melby, J.A. 1990. "Continued Monitoring of 42-Ton Dolos Movements and Static Stresses at Crescent City," American Society of Civil Engineers/WPCO Seminar on Stresses in Concrete Armor Units, New York.

_____. 1992. "Continued Monitoring of 42-Ton Dolos Movements and Static Stresses at Crescent City," Proceedings, 23rd ICCE, American Society of Civil Engineers, New York, NY.

Kobayashi, N., Wurjanto, A. 1990. "Numerical Prediction of Hydrodynamic Forces and Sliding Motion of Dolos Units." American Society of Civil Engineers/WPCO Seminar on Stresses in Concrete Armor Units, New York.

Markle, D.G. 1990a. "Physical Models of Coastal Structures as Designed and Used by the US Army Corps of Engineers," Journal of Coastal Research, Vol 5, No. 3, pp 573-592.

_____. 1990b. "Crescent City Instrumented Dolos Model Study," American Society of Civil Engineers/WPCO Seminar on Stresses in Concrete Armor Units, New York.

Markle, D.G., and Davidson, D.D. 1983. "Effects of Dolos Breakage on the Stability of Rubble-Mound Breakwater Trunks Subjected to Breaking and Nonbreaking Waves with no Overtopping," Technical Report CERC-83-4, US Army Engineer Waterways Experiment Station, Vicksburg, MS.

- McDougal, W. G., Melby, J. A., and Tedesco, J. T. 1987. "Wave Forces on Concrete Armor Units," Journal Waterway, Harbour, and Coastal Engineering Division, American Society of Civil Engineers, Vol. 114, No. WW5, pp 582-598.
- Melby, J. A. 1987. "Wave Induced Dynamic Response of Dolos Concrete Armor Units," Engineering Report, Oregon State Univ.
- Melby, J. A., and Howell, G. L. 1989. "Incorporation of Prototype Dolos Static Response in a Dolos Design Procedure," Proceedings, IAHR XXIII Congress, Ottawa, Canada.
- Melby, J. A., Rosson, B. T., and Tedesco, J. W. 1990. "An Analytical Investigation of Static Stresses in Dolosse," Journal of Waterway, Port, Coastal, and Ocean Engineering, American Society of Civil Engineers, Seminar on Stresses in Concrete Armor Units, New York.
- Melby, J. A., and Turk, G. F. 1992. "Dolos Design Using Reliability Methods," Proceedings, 23rd ICCE, American Society of Civil Engineers, New York.
- Merryfield, E. M., and Zwamborn, J. A. 1966. "The Economic Value of a New Breakwater Armor Unit Dolos," Proceedings, 10th Coastal Engineering Conference II, Sept., Tokyo, Japan, pp 885-912.
- Norman, C. D., and Alexander, A. M. 1985. "Measurement of Temperatures and Associated Strains During Dolosse Construction," Proceedings, Workshop on Measurement and Analysis of Structural Response in Concrete Armor Units, US Army Engineer Waterways Experiment Station, Coastal Engineering Research Center, Vicksburg, MS.
- Saucier, K. L. 1984. "High-Strength Concrete for Peacekeeper Facilities," Technical Report SL-84-3, US Army Engineer Waterways Experiment Station, Vicksburg, MS.
- Scott, D., Turcke, D., and Baird, W. F. 1990. "Structural Modeling of Dolos Armor Units," Journal Waterway, Harbour, and Coastal Engineering Division, American Society of Civil Engineering, Vol 116, No. 1, pp 120-136.
- Tait, R. B., and Mills, R. D. W. B. 1980. "An Investigation into the Material Limitations of Breakwater Dolosse," ECOR Newsletter No. 12.
- Tedesco, J. W., McGill, P. B., and McDougal, W. G. 1990. "Response of Prestressed Concrete Armor Units to Pulsating Loads," American Society of Civil Engineers/WPCO Seminar on Stresses in Concrete Armor Units, New York.
- Timco, G. W., and Mansard, E. P. D. 1982. "Improvements in Modelling Rubblemound Breakwaters," Proceedings, 18th ICCE, American Society of Civil Engineers, New York.
- US Army Corps of Engineers. 1985. "Stand practice for Concrete," Engineer Manual 1110-2-2000, Washington, DC.

van der Meer, J. W., and Pilarczyk, K. W. 1987. "Stability of Breakwater Armor Layers, Deterministic and Probabilistic Design," Delft Hydraulics Communication No. 378, Delft, The Netherlands.

Zwamborn, J. A., and Scholtz, J. D. P. 1986. "Dolos Armour Design Considerations," Proceedings, 20th ICCE, American Society of Civil Engineers, New York.

Zwamborn, J. A., Bosman, D. E., and Moes, J. 1980. "Dolosse; Past, Present, and Future." Proceedings, 17th ICCE, American Society of Civil Engineers, New York.

Zwamborn, J. A., Scholtz, J. D. P., and Claassens, H. 1988. "Stability and Structural Behavior of Strength Improved Dolosse," Proceedings, 21st ICCE, American Society of Civil Engineers, New York.

APPENDIX A: CAUDAID: Concrete Armor Unit Design Aid

Purpose

1. The purpose of this computer program is to predict the stress level and the resulting design factor of safety with respect to the fatigue reduced design strength in a dolos unit armor layer due to combined static and pulsating loads. The program is restricted to hydrodynamically stable dolos applications where only slight impact loads due to dolos rocking or projectiles within the armor layer are anticipated.

Background

2. The program CAUDAID automates the analytical approach contained in the dolos design procedure for computing the dolos stability and design stress. The program can be used to design dolosse for a wide variety of environmental and structural configurations, but it has only been validated for the Crescent City breakwater, where 42-ton dolosse with waist ratios of 0.32 are stacked in two or more layers on a 1:5 slope.

Program Description and Availability

3. This section contains a brief description of the program CAUDAID, version 2.0. The program CAUDAID runs on a personal computer (PC) under the DOS operating system. The program has been tested on a variety of PC systems. The installation instructions and late revision notes for the program are contained in a file called READ.ME on the distribution disk. The program contains context-sensitive help screens that can be accessed by pressing the ALT-H key combination. Version 2 of CAUDAID is currently in beta testing and a beta version of the program can be obtained directly from the author. Version 3 of the program, which is under development, will include results from dolos parametric physical model tests, dolos impact response, and reinforcement/strength enhancement optimization.

Program Layout

4. The program CAUDAID consists of two categories of subroutines: graphics screens and dolos design. The program contains five different types of graphics screens: title, data input, plotting menu, plots, and summary. The first screen is the title screen with the program name, the version number, the date of last revision, the author, and the publishing authority. The second screen is the data input screen. Values are required for dolos weight, unit weight or weight density, waist ratio, number of layers, fatigue factor, tensile strength, wave height, structure slope, stability coefficient, and design exceedance probability. The default values on this screen are those used for the 1986 Crescent City rehabilitation design, and the values input must be in English units. The choice of metric or English units will be added in a future release. The armor weight may be input as 0.0, in which case the program will compute the stable weight based on the Hudson equation. The user moves on to the next screen by pressing the F1 key, once all of the design values have been entered.

5. The third screen is the plot selection screen. This is a menu that allows the user to view various plots including waist ratio versus stress, layer versus stress, combined stress probability function, and design nomographs. The selected plot will then appear in the fourth screen. The user can view a summary output screen by choosing the SUMMARY option on this screen or can exit the program by choosing the selection. Again, the user moves to the next screen by pressing the F1 key.

6. The fourth screen is the plotting screen. This screen allows the user to view the stress relation and design plots and to interactively modify input data and view the results directly on the plots. This screen is the core of the program and can be used to optimize the dolos design for both hydrodynamic and structural stability. The screen has vertical and horizontal menus that provide the user with a wide variety of utilities. These utilities are described briefly in Tables A1 and A2.

7. The reader will note that the items in the horizontal menu can be selected by moving left and right using the cursor control keys or by pressing the key corresponding to the first letter of the menu item. Choosing the MENU item on the horizontal plot moves the cursor to the top of the vertical menu at the right side of the screen. The upper portion of the vertical menu is

Table A1
Screen 4 Horizontal Menu Item Descriptions

<u>Menu Item</u>	<u>Description</u>
SCAL	Modify the scales
GRID	Employ a grid
COLR	Change plot colors
STYLE	Change curve markers
LEGN	Relocate the legend
READ	Read points from curve
WIND	Zoom in on section of plot
EXC	Toggle exceedance line on and off
OUT	Select output device; screen, printer, plotter, file
QUIT	Exit program

Table A2
Screen 4 Vertical Menu Item Descriptions

<u>Menu Item</u>	<u>Description</u>
NEW GRAPH	Select new graph from previous screen
UPDATE GRPH	Update current graph with new values
MENU	Return to horizontal menu
UNIT WT	Dolos weight density, γ , in pcf
WEIGHT	Dolos total weight in tons
WAIST RATIO	Dolos waist ratio, $r = B/C$
LAYER	Number of armor layers
FATIGUE FAC	Fatigue factor strength reduction coefficient
STRENGTH	Dolos tensile splitting strength in psi
WAVE HEIGHT	Wave height, $H_{1/10}$, in ft
DESIGN EX %	Design probability of exceedance as %
FLUKE LEN	Dolos fluke length, C , in ft

used to return to the plot selection screen, redraw the current plot, or return to the horizontal menu. The lower portion of the vertical menu is provided so that the user can update the design variables and immediately see the effect on the design diagrams. To update a variable, the user simply moves the cursor to the variable and presses return. A program prompt will appear at the bottom of the screen. After the new value is entered, the user presses return, then moves the cursor to UPDATE GRAPH and again presses return. The plot will be updated with the new value.

8. Once the optimal design stress is computed in the fourth screen, the user can return to the plot selection screen and select SUMMARY. The fifth and final screen will then appear with the inputs and the associated design stress, factor of safety, and dolos dimensions. The user has the choice of writing the values on this screen to a file called CAUD.PRN, returning to the plot selection screen, or exiting the program.

Stress computation

9. The four dolos design subroutines consist of a control module and static, pulsating, and combined stress modules. The control module combines the stress subroutines with the graphics routines. The stress routines are all of the same nature, as follows. Each of the stress routines loads the probability density or ordinate array and the corresponding stress or abscissa array. The static nondimensional stress array is based on a modified log-normal distribution with the mean and standard deviation adjusted deterministically for waist ratio and the number of layers. The pulsating nondimensional stress array is computed using a Rayleigh distribution with the mean of the maximum stress computed using the average of the highest one-tenth waves. Each of the static and pulsating stress routines integrates the density function using a composite Simpson's rule. The step size for this integration is 0.333 and the number of steps is 600.

10. The combined stress routine is similar, except that the static and pulsating density functions are first convolved to achieve a single density function. This convolution is done using the composite Simpson's rule with a step size of 0.333, a lag size of 0.333, and a total of 600 steps. The resulting combined density function is then integrated to get a combined exceedance probability function, again using the composite Simpson's rule with 600 steps of size 0.333.

Design Example

11. Figure A1 shows an example of the SUMMARY screen output file called CAUD.PRN for the program default design values. The default values are from the 1986 Crescent City rehabilitation. Note that the design factor of safety is not conservative, even though there is no reduction in the strength to account for fatigue.

CAUDAID DOLOS STRUCTURAL DESIGN OUTPUT

DATE = 05/11/9
TIME = 10:33:29.70

DOLOS WEIGHT	42.00	tons
WAIST RATIO	0.32	
LAYERS	2.	
UNIT WEIGHT	155.00	pcf
STRENGTH	718.00	psi
FATIGUE COEF	1.00	
HUDSON Kd	16.00	ft
RUBBLE SLOPE	2.00	ft
WAVE HEIGHT	35.00	ft
DESIGN EXCEEDANCE	2. %	
DESIGN STRESS	970.99	psi
FACTOR-OF-SAFETY	0.74	
DOLOS DIMENSIONS	in inches	
A	36.43	
B	58.28	
C	182.13	
D	10.38	

Figure A1. Crescent City 1986 rehabilitation dolos design values as output from CAUDAID

12. Figures A2 through A5 show plots for this example. Note that the design nomograph shown in Figure A4 contains two solid curves and a dotted line. The solid curve increasing exponentially up to the right is the hydrodynamic stability curve based on the Hudson equation. Every point (H,W) to the right of this curve is hydrodynamically unstable, while those points to the left are stable. The solid curve sloping gently down to the right is the structural strength curve. Every point (H,W) above the strength curve

yields stresses in excess of the design stress level while those points below this curve are below the design stress level. Thus, the design envelope is the region to the left and below the solid stability curves. The point (H,W) at the apex of the dotted line represents the design wave height and dolos weight. Note that for the Crescent City dolosse, the design condition is slightly outside the design envelope. This could be corrected by increasing the waist ratio or by increasing the concrete strength.

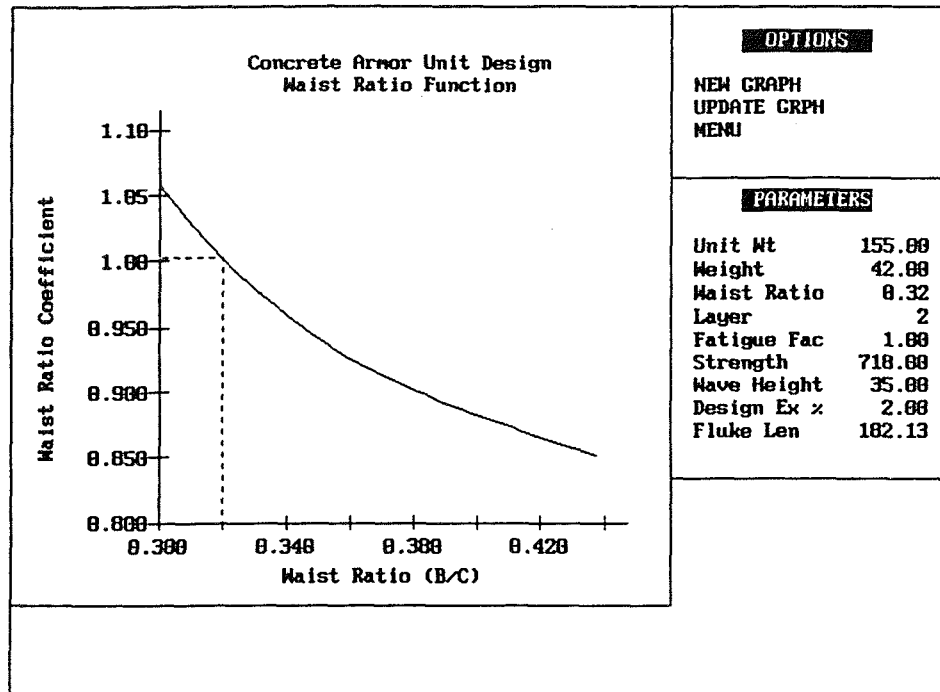


Figure A2. Dolos waist ratio versus stress coefficient as output from CAUDAID

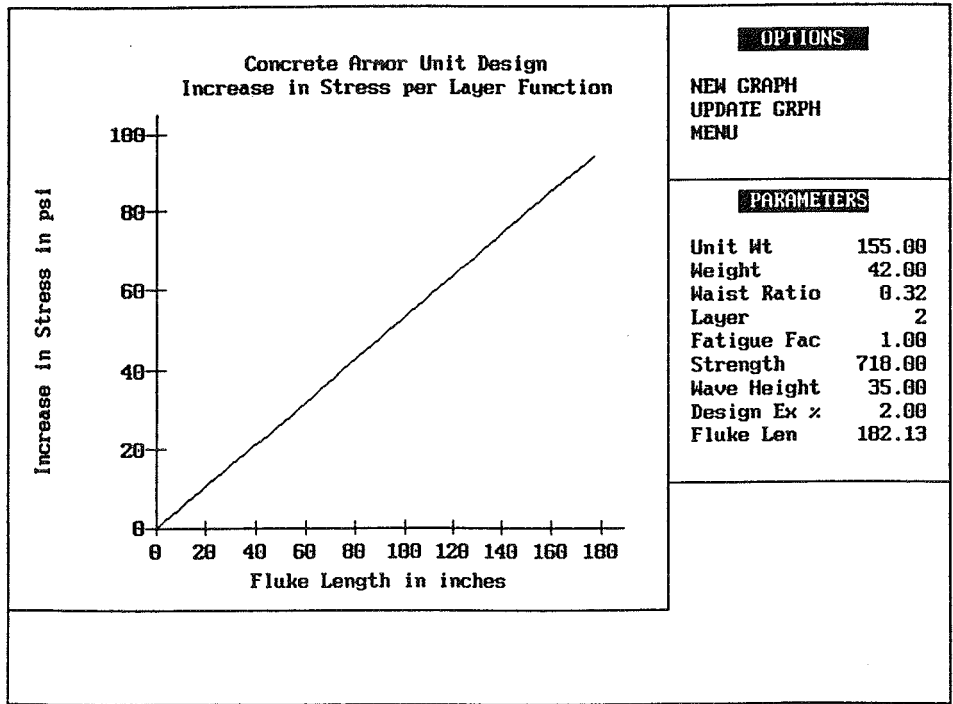


Figure A3. Dolos size versus added stress per layer as output from CAUDAID

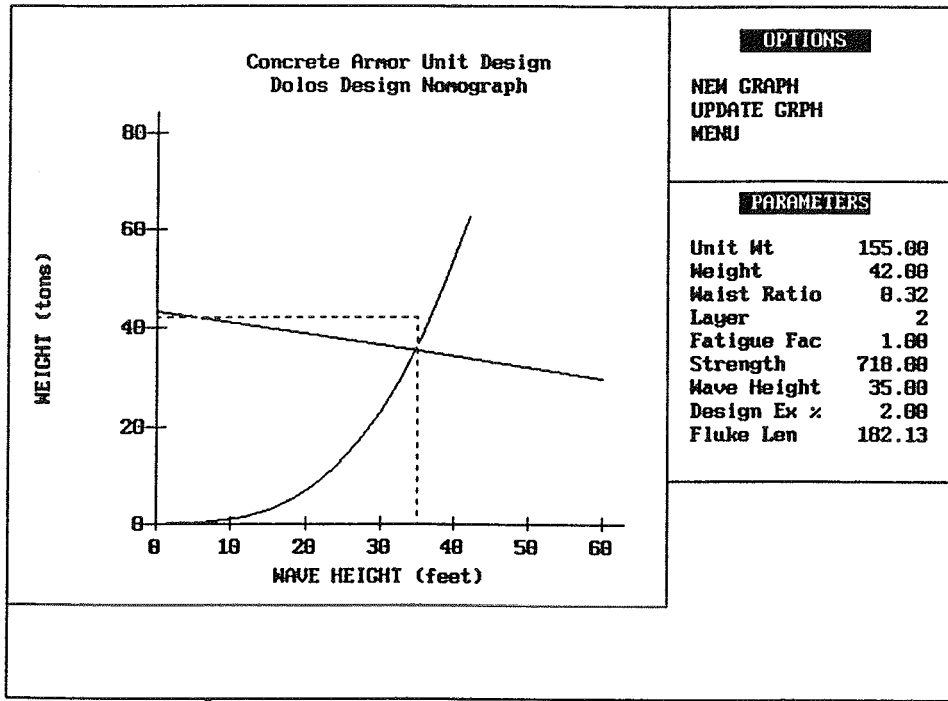


Figure A4. Dolos design nomograph as output from CAUDAID

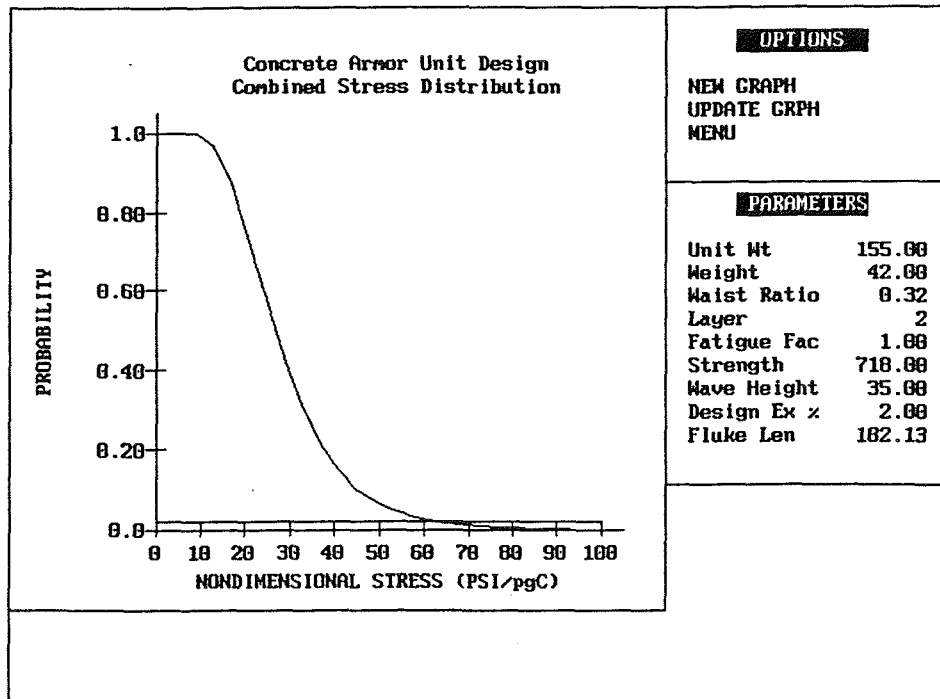


Figure A5. Dolos combined exceedance probability function as output from CAUDAID

APPENDIX B: NOTATION

α	Shift in static stress
A	Dolos fluke diameter at the fluke end
A	Cross-sectional area of shank
B	Dolos shank diameter
C	Dolos fluke length
C_{cc}	Crescent City dolos fluke length
D	Dolos chamfer dimension
cc	Subscript representing Crescent City prototype
f'_r	Concrete rupture tensile strength
f'_t	Concrete splitting tensile strength
FS	Factor of safety
g	Gravitational acceleration
h	Water depth
H	Wave height
$H_{1/10}$	Average of the 10 percent highest waves
I_x	Moment of inertia about x-axis
I_y	Moment of inertia about y-axis
k_F	Fatigue coefficient
k_{ps}	Wave stress constant
k_r	Waist ratio constant
k_{rL}	Waist ratio constant due to added layer
k_s	Wave stress constant
M_x	Moment about x-axis
M_y	Moment about y-axis
N_L	Number of dolos layers
p	Probability density
P	Exceedance probability
P	Axial load
r	Dolos waist ratio
S_L	Layer coefficient
t	Time
T	Wave period
W	Weight of dolos
x	Distance along x-axis from y-axis to neutral surface

y	Distance along y-axis from x-axis to neutral surface
α	Dolos static mean stress
α'	Nondimensional static mean stress
α''	Nondimensional adjusted static mean stress
β	Dolos static stress standard deviation
β'	Nondimensional static stress standard deviation
β''	Adjusted nondimensional static stress standard deviation
γ	Unit weight or weight density of dolos concrete
γ_{cc}	Unit weight of Crescent City dolos concrete
σ_{cc}	Dimensional Crescent City dolos static stress
σ'_{cc}	Nondimensional Crescent City static stress
$\bar{\sigma}'_{cc}$	Nondimensional Crescent City static stress mean
σ_p	Dimensional dolos pulsating stress
σ_{pmax}	Mean of maximum dimensional dolos pulsating stress
σ'_p	Nondimensional dolos pulsating stress
σ_s	Dimensional dolos static stress
σ_{sL}	Change in static stress per added layer
σ_s	Nondimensional dolos static stress
σ_{zz}	Dolos principal stress

REPORT DOCUMENTATION PAGE			Form Approved OMB No. 0704-0188	
Public reporting burden for this collection of information is estimated to average 1 hour per response, including the time for reviewing instructions, searching existing data sources, gathering and maintaining the data needed, and completing and reviewing the collection of information. Send comments regarding this burden estimate or any other aspect of this collection of information, including suggestions for reducing this burden, to Washington Headquarters Services, Directorate for Information Operations and Reports, 1215 Jefferson Davis Highway, Suite 1204, Arlington, VA 22202-4302, and to the Office of Management and Budget, Paperwork Reduction Project (0704-0188), Washington, DC 20503.				
1. AGENCY USE ONLY (Leave blank)	2. REPORT DATE June 1993	3. REPORT TYPE AND DATES COVERED Final report		
4. TITLE AND SUBTITLE Dolos Design Procedure Based on Crescent City Prototype Data			5. FUNDING NUMBERS	
6. AUTHOR(S) Jeffrey A. Melby				
7. PERFORMING ORGANIZATION NAME(S) AND ADDRESS(ES) USAE Waterways Experiment Station, Coastal Engineering Research Center, 3909 Halls Ferry Road, Vicksburg, MS 39180-6199			8. PERFORMING ORGANIZATION REPORT NUMBER Technical Report CERC-93-10	
9. SPONSORING/MONITORING AGENCY NAME(S) AND ADDRESS(ES) US Army Corps of Engineers Washington, DC 20314-1000			10. SPONSORING/MONITORING AGENCY REPORT NUMBER	
11. SUPPLEMENTARY NOTES Available from National Technical Information Service, 5285 Port Royal Road, Springfield, VA 22161.				
12a. DISTRIBUTION / AVAILABILITY STATEMENT Approved for public release; distribution is unlimited.			12b. DISTRIBUTION CODE	
13. ABSTRACT (Maximum 200 words) This design procedure includes statistical methods for determining a design stress in a dolos armor layer. The methods characterize the structural response as a single parameter: the maximum principal tensile stress in each dolos. Using this approach, the dolos shape can be optimized for structural integrity and hydrodynamic stability, and the design can be verified in the physical model. Also, the structural response to the most significant loading mechanisms can be computed separately and the individual statistical distributions combined to yield a design stress distribution. The design stress is computed using this design stress distribution and then compared to a fatigue-reduced strength. The iterative optimizing design process can be accomplished using a user-friendly PC-based computer program. It is shown that unreinforced normal-strength dolosse above 20 tons are often underdesigned with respect to strength and can tolerate only slight movement and the associated impacts. It is also shown that increasing the dolos waist ratio (Continued)				
14. SUBJECT TERMS Armor units Design Breakwater Dolos Concrete Hydraulic model			15. NUMBER OF PAGES 67	
			16. PRICE CODE	
17. SECURITY CLASSIFICATION OF REPORT UNCLASSIFIED	18. SECURITY CLASSIFICATION OF THIS PAGE UNCLASSIFIED	19. SECURITY CLASSIFICATION OF ABSTRACT	20. LIMITATION OF ABSTRACT	

13. ABSTRACT (Concluded)

can add significantly to the unit's strength, while sacrificing little hydrodynamic stability, and that large dolosse over 30 tons require some strengthening scheme. The methods discussed in this paper provide a complete procedure for determining a design stress within a hydrodynamically stable dolos and can be used as an outline in the design of other slender armor unit shapes.